

Alma Mater Studiorum Università di Bologna
Archivio istituzionale della ricerca

Structurally controlled growth of fibrous amphibole in tectonized metagabbro: constraints on asbestos concentrations in non-serpentinized rocks

This is the final peer-reviewed author's accepted manuscript (postprint) of the following publication:

Published Version:

Vignaroli, G., Rossetti, F., Billi, A., Theye, T., Belardi, G. (2020). Structurally controlled growth of fibrous amphibole in tectonized metagabbro: constraints on asbestos concentrations in non-serpentinized rocks. JOURNAL OF THE GEOLOGICAL SOCIETY, 177(1), 103-119 [10.1144/jgs2018-235].

Availability:

This version is available at: <https://hdl.handle.net/11585/711199> since: 2020-01-01

Published:

DOI: <http://doi.org/10.1144/jgs2018-235>

Terms of use:

Some rights reserved. The terms and conditions for the reuse of this version of the manuscript are specified in the publishing policy. For all terms of use and more information see the publisher's website.

This item was downloaded from IRIS Università di Bologna (<https://cris.unibo.it/>).
When citing, please refer to the published version.

(Article begins on next page)

This is the final peer-reviewed accepted manuscript of:

Vignaroli, Gianluca and Rossetti, Federico and Billi, Andrea and Theye, Thomas and Belardi, Girolamo, Structurally controlled growth of fibrous amphibole in tectonized metagabbro: constraints on asbestos concentrations in non-serpentinized rocks, (2020) *Journal of the Geological Society*, 177 (1), pp. 103-119

The final published version is available online at: <https://doi.org/10.1144/jgs2018-235>

Terms of use:

Some rights reserved. The terms and conditions for the reuse of this version of the manuscript are specified in the publishing policy. For all terms of use and more information see the publisher's website.

This item was downloaded from IRIS Università di Bologna (<https://cris.unibo.it/>)

When citing, please refer to the published version.

Accepted Manuscript

Journal of the Geological Society

Structurally controlled growth of fibrous amphibole in tectonised metagabbro: constraints on asbestos concentration in non-serpentinised rocks

Gianluca Vignaroli, Federico Rossetti, Andrea Billi, Thomas Theye & Girolamo Belardi

DOI: <https://doi.org/10.1144/jgs2018-235>

Received 30 December 2018

Revised 15 June 2019

Accepted 12 August 2019

© 2019 The Author(s). Published by The Geological Society of London. All rights reserved. For permissions: <http://www.geolsoc.org.uk/permissions>. Publishing disclaimer: www.geolsoc.org.uk/pub_ethics

To cite this article, please follow the guidance at http://www.geolsoc.org.uk/onlinefirst#cit_journal

Manuscript version: Accepted Manuscript

This is a PDF of an unedited manuscript that has been accepted for publication. The manuscript will undergo copyediting, typesetting and correction before it is published in its final form. Please note that during the production process errors may be discovered which could affect the content, and all legal disclaimers that apply to the journal pertain.

Although reasonable efforts have been made to obtain all necessary permissions from third parties to include their copyrighted content within this article, their full citation and copyright line may not be present in this Accepted Manuscript version. Before using any content from this article, please refer to the Version of Record once published for full citation and copyright details, as permissions may be required.

Structurally controlled growth of fibrous amphibole in tectonised metagabbro: constraints on asbestos concentration in non-serpentinised rocks

Gianluca Vignaroli^{1,*}, Federico Rossetti², Andrea Billi³, Thomas Theye⁴, Girolamo Belardi⁵

¹ Dipartimento di Scienze Biologiche, Geologiche e Ambientali, Università di Bologna, Via Zamboni, 67, 40126 Bologna, Italy

² Dipartimento di Scienze, Sezione di Geologia, Università degli Studi di Roma Tre, Largo S.L. Murialdo, 1, 00146 Rome, Italy

³ Consiglio Nazionale delle Ricerche, c.o. Dipartimento di Scienze della Terra, Sapienza Università di Roma, P.le Aldo Moro 5, 00185 Roma, Italy

⁴ Institut für Mineralogie und Kristallchemie, Universität Stuttgart, Azenbergstr. 18, D-70174, Stuttgart, Germany

⁵ Consiglio Nazionale delle Ricerche, Istituto di Geologia Ambientale e Geoingegneria (CNR-IGAG), Via Salaria km 29,300 - 00015 Monterotondo, Rome, Italy

* Corresponding author:

G. Vignaroli

Dipartimento di Scienze Biologiche, Geologiche e Ambientali
Università di Bologna

Via Zamboni, 67 - 40126 Bologna, Italy

gianluca.vignaroli@unibo.it

Abstract

Asbestos nucleation and concentration in rocks are mostly associated with mechanisms of fibre formation, combined with the water-dependent mineralogical alteration produced during serpentinisation of ultramafic masses. Very little is known about the structural settings and tectonic histories that influence and control asbestos occurrence in non-serpentinised rocks, which are diffusely embedded within tectonised ophiolitic suites. Focussing on a case history provided by a tectonised metagabbro from the Ligurian Alps (northern Italy), a multiscale structural-petrographical approach is used to investigate the relationships between rock fabric and fibrous amphibole growth within the metagabbro. Meso- to micro-structural observations are used to document the role of structurally controlled fluid-rock interactions in localising the fibrous amphibole growth during ductile-to-brittle shearing (mylonitic foliation to shear veins). A qualitative structural scenario is here provided for illustrating the growth of asbestos amphiboles in shear veins during the progression of shear deformation towards semi-brittle rheological conditions. The mechanisms of structurally controlled growth of fibrous amphibole in non-serpentinised rocks imply an examination of the tectonic boundary conditions that are at the origin of the asbestos concentration in ophiolitic rocks involved in orogenic belt construction.

Key words: rock fabric, vein, amphibole, asbestos, metagabbro, serpentinite, Ligurian Alps.

The causes of asbestos hazard in natural environments include production and dispersion of airborne particles during natural (erosion) and/or anthropogenic activities (e.g., construction, grading, quarrying, and surface mining operations) involving ophiolitic lithotypes (e.g., Rohl *et al.*, 1977; Pan *et al.*, 2005; Gunter *et al.*, 2007; Lee *et al.*, 2008). Presently, stringent requirements for rock quality control and regulations are required to mitigate the asbestos hazard in natural settings (Clinkenbeard *et al.*, 2002; Lee *et al.*, 2008), as asbestos is listed as a Group 1 human carcinogen material by international health authorities (Ross *et al.*, 1984; WHO, 1986; International Agency for Research on Cancer [IARC], 1987; 2012; Health and Safety Executive, 1997; National Institute for Occupational Safety and Health [NIOSH], 2011).

The wide range of asbestos concentration, from only episodic occurrences to large deposit accumulations, has been documented worldwide in serpentinite rocks (e.g., Ross and Nolan, 2003; Van Gosen, 2007; Hendrickx, 2009; Bloise *et al.*, 2017). The water activity-dependent mineralogical alteration produced during serpentinisation of ultramafic rocks, controlled by the general reaction



is considered the main process triggering the asbestos growth in the form of chrysotile (Mooby, 1976; O'Hanley, 1996).

Chrysotile growth depends on several factors, such as thermo-barometric conditions of the whole rock ($T < \sim 400^\circ\text{C}$ with negligible P effect; e.g., Evans, 2004; Bucher and Grapes, 2011), fluid infiltration and interaction with the host rocks (Bellot, 2008), and mechanisms of fibre formation, which include (i) re-orientation of pre-existing fibres (Reinen, 2000), (ii) physico-chemical dissolution and replacement of early clasts by micro-scale shearing (Andreani *et al.*, 2005; Hirauchi and Yamaguchi, 2007), and (iii) crack-seal vein growth (see discussion in Groppo and Compagnoni, 2007). The fibre formation is closely related to the development of both ductile (mylonites) and brittle (veins) deformation structures, as documented both by studies of tectonically deformed serpentinites and laboratory experiments (e.g., Phillips, 1927; Gabrielse, 1960; Wicks and Wittaker, 1977; Hoogerduijn Strating and Vissers, 1994; Karkanias, 1995; Hermann *et al.*, 2000; Reinen, 2000; Andreani *et al.*, 2004; 2005; Auzende *et al.*, 2006; Boschi *et al.*, 2006; Hirose *et al.*, 2006; Groppo and Compagnoni, 2007; Hirauchi and Yamaguchi, 2007; Viti and Hirose, 2009; Viti *et al.*, 2011). Feedbacks and interactions between polyphase deformation, decompression/cooling, and fluid circulation enhance the fibrous mineralisation in serpentinites (Trommsdorff and Evans, 1974; Evans, 1977; Cox and Etheridge, 1983; Norrell *et al.*, 1989; Hoogerduijn Strating and Vissers, 1994; Andreani *et al.*, 2005; 2007; Auzende *et al.*, 2006; Vignaroli *et al.*, 2011).

Nevertheless, non-serpentinised rocks (i.e., rock volumes that did not experience diffuse serpentine-bearing mineralogical replacement) are also known to host asbestos as accessory

minerals, typically grown in specific structural sites like veins (e.g., Taber, 1918; Gianfagna *et al.*, 2003; Ross and Nolan, 2003; Boschi *et al.*, 2006; Compagnoni and Groppo, 2006; Van Gosen, 2007; Giacomini *et al.*, 2010; Vignaroli *et al.*, 2014; Punturo *et al.*, 2015; Lucci *et al.*, 2018). Non-serpentinised rocks often occur as tectonic blocks (of various sizes) in ophiolitic suites that have experienced chronologically distinct tectono-metamorphic events associated with the subduction-exhumation cycles (Coleman, 1977; Scambelluri *et al.*, 1991; Hermann *et al.*, 2000; Li *et al.*, 2004; Cawood *et al.*, 2009). Multiple events of fluid-assisted deformation and metamorphism provide an ideal tectonic scenario to frame the structurally controlled growth of secondary mineralisation, including different varieties of asbestos. However, as compared to the study of naturally occurrence asbestos in serpentinites, little attention has been devoted to geological factors leading to asbestos growth and its resulting concentrations in non-serpentinised rocks. In particular, the following key questions remain unanswered: (i) what are the key structural factors (primary and secondary) leading to fibrous growth in non-serpentinised rocks? and (ii) which are the main boundary conditions that trigger the growth of fibrous minerals during the development of the secondary (tectonic) rock fabrics?

In order to better understand the structural processes controlling fibrous amphibole crystallisation in non-serpentinised rocks, we studied the deformation fabric (from outcrop-, to meso- and micro-scales) of a km-scale metagabbro outcrop in the Ligurian Alps (northern Italy; Figs. 1a, b). Correlation between deformation fabric progress and fibrous amphibole nucleation/concentration is recognised. The major novelty of this work is the documentation of textural heterogeneities and structurally controlled secondary permeability development over the nucleation and development of amphibole fibres in the transition from ductile- to brittle-dominated deformation environments. The results are used to move from site-specific evidence to general concepts, in order to propose a qualitative scenario for feedbacks and interactions of geological factors at the origin of asbestiform mineralisations in tectonised ophiolitic rocks involved in orogenic belt construction.

1. Materials, Methods and Definitions

This study focuses on a huge metagabbro body continuously exposed over about 2 km² (Fig. 1c). Meso-scale structural and petrographical investigations were used to characterise the key structural heterogeneities of the rock fabric (such as tectonic foliation, veins, fractures, and fault systems). Rock samples representative of the range of lithotypes, the deformation structures, and the

mineralisation (Table 1) of this body were collected for microtextural investigations to define: (i) the textural sites of amphibole nucleation and growth; (ii) the morphological habit of amphibole crystals (i.e., massive vs. fibrous); (iii) the mode of fibre growth (i.e., individual or in bundles); and (iv) the textural relationships between fibre nucleation and the surrounding fabrics.

We analysed the amphiboles based on: (i) their morphological parameters (i.e. length, width, shape, and cleavage type) by combining optical transmitted-light microscopy and scanning electron microscopy (SEM); and (ii) their chemistry by combining electron microprobe analyses (EMPA) and concentration maps for major elements (i.e., Fe, Mg, Ca, and Al). The amphibole composition was measured using a Cameca SX100 electron microprobe at the Universität Stuttgart. Analyses were performed in focussed-beam mode at 15 kV and 10 to 15 nA using natural minerals and synthetic phases as standards. Mineral recalculation and estimation of Fe^{3+} contents were made using the WinAmphcal software (Yavuz 2007), normalising to 15 cations and O=23. Amphiboles were classified according to the nomenclature approved by the International Mineralogical Association (Leake *et al.*, 2004). Major elemental (Ca, Fe, Mg, and Al) maps showing relative concentrations were produced by stepwise movements of the thin sections under the electron beam. The mineral abbreviations used in this work are after Bucher and Grapes (2011).

After terminology re-examination based on accepted standards and several research works (e.g., Asbestos Hazardous Emergency Response Act [AHERA], 1987; Occupational Safety and Health Administration [OSHA], 1994; World Health Organization [WHO], 1986; Dorling and Zussman, 1987; Gunter *et al.*, 2007; Strohmeier *et al.*, 2010; ASTM D7712-11, 2011), the following definitions are used in this paper:

- Asbestiform is used for a special type of mineral fibrous morphology, typical of asbestos, in which the fibres are separable into thinner fibres and ultimately into fibrils.
- Asbestos is used for six specific silicate minerals belonging to the serpentine (chrysotile) and amphibole (riebeckite - crocidolite; grunerite - grunerite asbestos; anthophyllite - anthophyllite asbestos; tremolite - tremolite asbestos; and actinolite - actinolite asbestos) groups. Asbestos crystallises in the asbestiform habit, where crystals can be easily separated into long, thin, flexible, and strong fibres when crushed or processed.
- Fibre is used for an elongated particle, longer than 5.0 μm , with a minimum aspect ratio (length of the particle divided by its width) of 3:1. Fibres are characterised by parallel or stepped sides developed during growth.

- Fibril is used for a single fibre that cannot be further separated longitudinally into smaller components without losing its fibrous properties or appearances.
- Fibrous is used for a crystal morphology that exhibits parallel, radiating, or matted aggregates of fibres.

2. The geological setting of the study area

The investigated metagabbro body is located in the eastern part of the Ligurian Alps (Italy), a narrow E-W-trending mountain belt connecting the Western Alps to the Northern Apennines (Fig. 1a). The Ligurian Alps are characterised by the occurrence of plurikilometre-sized meta-ophiolitic units that are remnants of the Jurassic oceanic crust of the Liguro-Piedmont Domain (e.g., Chiesa *et al.*, 1975; Piccardo, 2012). This ocean was subducted and exhumed during the Cretaceous-Tertiary Alpine tectonic convergence between the European and Adriatic plates (e.g. Vanossi *et al.*, 1984). The Ligurian meta-ophiolites define a tectonic *mélange* of huge masses of serpentinites incorporating blocks and slices (of different sizes) of eclogites, metagabbros, and metabasalts, with associated calcschists and micaschists (Fig. 1b). The ophiolites underwent subduction zone metamorphism during the Alpine orogeny, ranging from greenschist to eclogite facies conditions, (e.g., Messiga and Scambelluri, 1991; Capponi and Crispini, 2002; Vignaroli *et al.*, 2005; 2010; Federico *et al.*, 2007a). The ophiolites are characterised by a polyphase deformation fabric that records the progressive evolution from ductile high-pressure shearing to late, multistage, brittle deformation (e.g., Hoogerduijn Strating, 1994; Capponi and Crispini, 2002; Cannà *et al.*, 2016).

Most of the boundaries between serpentinites and the embedded rock blocks are tectonic and systematically marked by steeply dipping shearing fabrics, including pervasive mylonitic shear zones and polyphase vein systems (Hermann *et al.*, 2000; Federico *et al.*, 2007a; 2007b; Vignaroli *et al.*, 2009; Malatesta *et al.*, 2012). Brittle deformation often overprints the ductile fabric, with development of high-angle faults and associated fracture networks reworking the ductile boundaries (e.g., Crispini *et al.*, 2009; Federico *et al.*, 2009; Vignaroli *et al.*, 2009). Evidence of progressively refolded mylonitic zones with superimposed brittle deformation features testifies for the polyphase exhumation of the originally deep-seated ophiolite units in a continuum from deep to upper crustal levels (e.g., Hoogerduijn Strating, 1994; Crispini and Frezzotti, 1998; Capponi and Crispini, 2002; Vignaroli *et al.*, 2010).

Such a polyphase tectono-metamorphic history is well documented by the ductile-to-brittle tectono-metamorphic fabric recorded by several oceanic-derived magmatic bodies, wrapped around by the sheared serpentinite masses (Federico *et al.*, 2007a; Malatesta *et al.*, 2012). Heterogeneous strain and metamorphic overprints are recorded by the tectonic blocks (Messiga and Scambelluri, 1991; Vignaroli *et al.*, 2005; Federico *et al.*, 2007b; Malatesta *et al.*, 2012).

3. Fabric analysis

3.1 Outcrop scale

The investigated metagabbro forms a km-scale (~ 2 km-long and 0.5 km-large) N-S elongate tectonic block (Fig. 1b). The main tectonic foliation is subvertical, synkinematic relative to a pervasive greenschist metamorphism. Ductile foliation is cut across by high-angle fault and vein systems (Fig. 1c).

The selected rock exposures (Fig. 2) include the distinctive primary (igneous) and secondary (tectonic) fabrics of the metagabbro body. The primary igneous fabric is defined by the mineral assemblage made of clinopyroxene and plagioclase aggregates (sample TB62; Table 1 and Fig. 2a), with variable grain size, from fine- (sub-to-mm scale) to coarse-grained (cm scale). The tectonic fabric is metamorphic and syn-kinematic relative to a pervasive greenschist facies stage (e.g., Capponi and Crispini, 2002; Federico *et al.*, 2007b). The metamorphic overprint is attested by the (i) pseudomorph replacement of igneous clinopyroxene by amphibole; and (ii) the development of meso-scale ductile shear zones, associated with syn-metamorphic intrafoliar, millimetre-thick, amphibole-quartz veining. The ductile shearing is distributed in discrete (up to 5 m thick) horizons that show evidence of penetrative secondary foliation development and strain accumulation (foliated metagabbro; sample TB59; Table 1 and Fig. 2b). The shear foliation shows an anastomosed geometry around the pristine magmatic clinopyroxene porphyroclasts (Fig. 2c). The shear foliation, striking N100° and dipping toward SSW, consists of a composite layering of dominant plagioclase-rich and green amphibole-rich layers, with subordinate chlorite, epidote, and oxides. Both the plagioclase-rich and amphibole-rich layers show finer grain sizes than the porphyroclastic clinopyroxene.

Semi-brittle to brittle deformation fabrics overprint the previously described ductile rock fabrics. These structures are represented by shear veins and joints that cut at a high angle (>50°) and post-dates the shear foliation. This vein pattern is highly persistent (shear veins are 2–3 cm-thick and up to 10 m in length) and characterised by a spacing ranging from 0.5 to 2–6 m (Fig. 2d). A mineralogical association of plagioclase and quartz with occasional occurrences of fibrous

amphiboles is found within the shear veins (sample TB61; Table 1). Whitish to green amphibole fibres, which are up to 2 cm in length (measured from the vein surface), are observed to protrude from the coarse-grained plagioclase assemblage (Figs. 2e-f).

3.2 *Microscale*

We present a description of the microstructural characteristics of the metagabbro from observations of three selected thin sections (Fig. 3), each one representative of the fabric types recognised at the outcrop scale.

The massive metagabbro (sample TB62) shows a fine-grained texture without any evidence of secondary foliation (Fig. 3a). The grains of the groundmass are up to half a millimetre in diameter and consist mainly of magmatic clinopyroxene and plagioclase (Fig. 4a). Magmatic clinopyroxene is mostly isomorphic in shape and with abundant internal microcracks filled by alteration products. Amphiboles, in association with plagioclase, form a fine matrix around the clinopyroxene grains and, occasionally, fill the microcracks (Figs. 4b, c).

The mylonitic fabric in foliated metagabbro (sample TB59) shows a penetrative mineralogical banding of stretched aggregates of neocrystallised amphiboles and elongated aggregates of neocrystallised fine-grained albitic plagioclase (Fig. 3b). The mylonitic foliation shows a dominant plane-parallel geometry, locally evolving into an anastomosed geometry where fractured clinopyroxene porphyroclasts are wrapped around. Amphiboles grow in two distinct microsites: (i) along the mylonitic foliation (Figs. 5a-c), and (ii) in pressure shadows surrounding the clinopyroxene porphyroclasts (Figs. 5d-f).

The shear veins (sample TB61) that post-date the mylonitic foliation are filled by dominant coarse-grained plagioclase and subordinate quartz (Fig. 3c). The interface between the veins and the metagabbro is very sharp and almost rectilinear. This interface truncates the mylonitic foliation at a high angle. Finer plagioclase grains are disposed close to the interface, whereas coarser grains occur towards the centre of the vein. Plagioclase grains are arranged in an elongate-blocky texture, showing evidence of growth competition (e.g., Vernon, 2004). Amphiboles grow in two distinct microsites: (i) at the vein/metagabbro interface that truncates the syn-greenschist foliation (Fig. 6a), and (ii) at the vein/metagabbro interface that truncates the porphyroclastic clinopyroxene (Figs. 6b, c). Amphiboles (fibrous or otherwise) do not form along the interface of the vein with fine-grained massive metagabbro (Figs. 6d, e). On the other hand, fibrous amphibole can occur within intrafoliar vein in massive metagabbro (Fig. 6d).

3.3 Micro-structures hosting amphibole crystallisation

Mylonitic foliation (Figs. 5a-c). The mylonitic foliation consists of aggregates of amphibole neoblasts that show a brownish to yellowish, to light green pleochroism, and homogeneous extinction under crossed polarised light. In particular, foliated aggregates of amphiboles form thin (up to 50 μm), sub-parallel C-type shear bands, whereas fan-shaped aggregates of amphiboles form an oblique (S-type) foliation (Fig. 5a). The back-scatter electron (BSE) imaging of the C-type shear bands reveals elongate (prismatic-to-lanceolate) amphiboles, with width and length ranging between 3-20 μm and 10-200 μm , respectively, texturally in contact with grains of plagioclase and oxides (Fig. 5b). The most elongated amphibole particles show rectilinear and parallel sides with edges that are mostly smooth or gently curved. Edges with irregular shapes and fibrous terminations are less common.

Corona textures (Figs. 4a-c and 5d-f). Coarse-grained clinopyroxene porphyroclasts show evidence of mineralogical replacement at their grain margins (Figs. 4b and 5d). These replacement halos are marked by a series of adjacent/coalescent lobes made of plagioclase and brownish-to-yellowish amphibole. BSE images show that the amphiboles form massive assemblages (Figs. 4b and 5e). The amphiboles, which formed as product of the clinopyroxene alteration, show a dominant prismatic morphological habit with basal section rarely visible. The edges of the amphiboles are very irregular and have no evidence of fibrous terminations.

Shear Veins. We observed three microtextures: (i) veins cutting through the mylonitic foliation (Fig. 6a), (ii) veins cutting through magmatic relicts (Figs. 6b, c), and (iii) veins cutting through the fine-grained massive groundmass (Figs. 6d, e). In the veins cutting through the mylonitic foliation (Fig. 6a), amphiboles occur exclusively in microsites where the veins truncate the amphibole-rich foliation in the host rock. Amphiboles nucleate at the vein/metagabbro interface and show an extremely fibrous habit. The fibres are very thin (their width is less than 5 microns) and long (up to 1 millimetre) and are organised as either individual specimens or bundle structures. Optically, the fibres have brownish to yellowish to light green pleochroism, and homogeneous extinction under crossed polarised light.

In veins cutting through magmatic porphyroclasts (Figs. 6b, c), amphiboles occur at the microsites where the veins truncate coarse-grained clinopyroxene. From a morphological point of view, amphiboles grow extremely fibrous enclosed in relatively coarse-grained plagioclase. The fibres of amphiboles are brownish to yellowish in colour, with homogeneous extinction under crossed polarised light (Figs. 7a-c). They are organised as either individual specimens or bundle

structures. Each fibre has a dominant rectilinear shape (sometimes slightly curved) that is oriented perpendicular to the trend of the vein wall (Figs. 7d, e). Fibre terminations show individual smaller fibres (fibrils) disseminated within the plagioclase matrix (Fig. 7f). By contrast, the amphiboles that grow as filling material for clinopyroxene microcracks is not fibrous and does not show a clear crystallographically preferred orientation with respect to the host clinopyroxene (Fig. 7g). Here, the amphiboles show an elongated prismatic morphological habit, but no individual fibres of amphiboles occur.

It is interesting to note a geometrical parallelism between the orientation of cleavage within the truncated clinopyroxene and the trend of the fibrous amphiboles (Figs. 8a, b). In other words, the *c* axes of clinopyroxene and amphibole often coincide even across interfaces between relic clinopyroxene and vein formations. BSE imaging reveals that the site of nucleation of each fibre corresponds to strongly cleaved microdomains of clinopyroxene. The fibres are very thin (their width is less than 5 microns) and long (more than 1 millimetre).

Finally, in veins cutting through the fine-grained massive groundmass (Fig. 6e), neither massive nor fibrous amphiboles nucleate on the vein-metagabbro interface. We observed fibrous amphiboles as the main filling component of microveins within the fine-grained metagabbro fabric (similar to that described in the above sub-paragraph; Fig. 6b), but no amphiboles developed within the plagioclase-quartz vein (Fig. 6c). At the vein margins, the growth competition textures of elongate plagioclase grains can be observed.

4. Amphibole chemistry

We distinguish the amphibole types based on their structural/textural setting and on their chemical composition (Fig. 9). Average chemical compositions of the analysed amphiboles are reported in Table 2. All analysed grains are calcic amphiboles ($\text{Ca}_B > 1.50$; Leake *et al.*, 2004). Amphiboles marking the mylonitic foliation (Fig. 5a) and those ones found in corona structures (Figs. 4b and 5e) both show moderate variability in Si^{4+} contents (ranging from 7.00 to 7.90 atoms per unit formula). According to the $\text{Mg}/(\text{Mg}+\text{Fe}^{2+})$ ratio, these amphiboles define two populations falling in the Mg-hornblende and actinolite fields. Conversely, the amphiboles grown in shear veins (Figs. 6a, b) show a more homogeneous composition falling within the actinolite field (average $\text{Si}^{4+} = 7.89$ atoms per unit formula; average $\text{Mg}/(\text{Mg}+\text{Fe}^{2+}) = 0.75$).

Elemental concentration maps reveal that different amphibole types are characterised by a rather homogeneous distribution for Fe, Mg, Ca, and Al along a single crystal. Indeed, amphiboles in corona structures do not show appreciable chemical zoning (Figs. 4c and 5f). Similarly, no chemical zoning is discernible in both amphiboles marking the shear foliation (Fig. 5c) and amphiboles in shear veins (Figs. 8a, b).

5. Discussion

5.1 Rock fabric and occurrence of fibre-hosting structures: a structural synthesis

Within the tectonised metagabbro fabric, we identify two main structurally controlled types of amphibole crystallisation (Fig. 10): (i) diffuse growth in ductile shears (Type-1 in Fig. 10); and (ii) localised growth in shear veins (Type-2 in Fig. 10).

Type-1 growth corresponds to the syn-greenschist metamorphic overprint of the primary igneous fabric under ductile deformation conditions. The structurally controlled sites of amphibole crystallisation consist of: (i) corona structures around clinopyroxene porphyroclasts; (ii) clinopyroxene internal microcracks; and (iii) mylonitic foliation. While both the corona structures (Figs. 4b and 5e) and the clinopyroxene internal microcracks (Fig. 7g) represent low-strain rock micro-domains hosting massive assemblages of prismatic amphibole, the mylonitic foliation defines a penetrative deformation structure hosting amphibole crystallisation within the dominant elongate habit (Fig. 5a). In particular, aggregates of neocrystallised amphiboles (whose composition is transitional from Mg-hornblende to actinolite) contribute to the formation of the C-type shear bands (Fig. 5b). This dominant syn-kinematic growth of fibrous amphibole along the mylonitic foliation suggests dynamic growth along planes of maximum shear deformation, analogous to slickenfibre development (Shelley, 1994). The passive re-orientation of former fibres as rigid elements (Reinen, 2000) seems not to be a possible mechanism, as no amphibole fibres were observed pre-dating the syn-greenschist mylonitic foliation.

Type-2 growth corresponds to the syntaxial growth of the shear veins post-dating the greenschist foliation. The textural evidence attesting for the syntaxial growth includes (e.g., Vernon, 2004; Passchier and Trouw, 2005; see Bons *et al.*, 2012): (i) growth competition textures of elongate plagioclase crystals nucleated along the vein/metagabbro interface; (ii) growth direction from the vein walls towards the vein centre; (iii) coarsening of the plagioclase grains moving from the walls to the vein centre; and (iv) fibres of amphiboles (actinolite composition) nucleated at the

vein-metagabbro interface and penetrating the plagioclase mass. Fibres nucleated exclusively at specific microsites, corresponding both to intersections between veins and amphibole-rich foliations (Fig. 6a) and those between veins and clinopyroxene grains (Fig. 7a), suggesting an active control of inherited textures in forming fibrous amphiboles. The nucleation of fibres from the vein walls in correspondence of truncated mafic minerals suggests a dominant dissolution-diffusion-crystallisation (Andreani *et al.*, 2005). Possibly, the crack-seal mechanism could be attributed to the latest stages of vein opening, when the (quasi) static crystallisation of plagioclase fills the dilatant space forming an elongated blocky texture.

To summarise, the Type-1 and Type-2 growth scenarios demonstrate the structural control of fibrous growth in the transition from ductile- to brittle-dominated deformation environments. We frame the structural control over fibrous mineralisation within the complete rock-failure criterion for ductile and brittle regimes (e.g., Twiss and Moores, 2007; Davis *et al.*, 2011), with the aim of explaining how the formation of these fibre-hosting structures responded to the critical stress conditions at which the metagabbro rock volume deformed (Fig. 11). Mylonitic foliation (Type-1) formed at high confining pressures (named σ_{1a} and σ_{3a} in Fig. 11), at which the plastic yielding is regulated by the von Mises criterion for rock failure (Fig. 11). We therefore suggest that elongate crystals of amphibole grow along surfaces of ductile failure (C-type shears) where the maximum shear stress was localised during the greenschist metamorphic conditions. The superimposition of Type-2 brittle fabric (shear veins) on the mylonitic foliation suggests that the rock volume experienced failure at lower confining pressure conditions (named σ_{1b} and σ_{3b} in Fig. 11). This new state of stress may have been reached by a lowering of the mean stresses, which was probably due to the progressive exhumation of the rock volume. In particular, the Type-2 shear veins formed through a hybrid mode of opening (Hancock, 1985; Ramsey and Chester, 2004; Bons *et al.*, 2012). The Mohr-Coulomb failure criterion considers a hybrid failure under the conditions of negative minimum principal stress. The conditions of negative stress can occur in the presence of elevated fluid pressure (P_f), which contrasts with the confining pressure by lowering the differential stress necessary to cause failure (Cox *et al.*, 2001; Sibson, 2004; Cox, 2010). This results in shifting the Mohr circle towards lower mean stresses by an amount equal to the P_f (σ_{1c} and σ_{3c} in Fig. 11). Failure by hybrid mode rules out the re-shear mechanism along an early cohesionless fabric, suggesting that the rock volume was intact when the veining took place. Therefore, it is possible to consider the Type-2 shear veins as structures favoured by pore overpressure and mineralising fluid discharge (Cox *et al.*, 2001; Sibson, 2004; Cox, 2010). We suggest that amphibole fibre growth occurred within these fluid-driven structures as a sealing mineral material in a fluid-pressure-cycling scenario.

5.2 Insights on asbestos growth in non-serpentinised rocks

The scenario described above suggests that fibrous mineralisation in the studied metagabbro provide insights on the naturally occurring asbestos in non-serpentinised rocks (e.g., Ross and Nolan, 2003; Compagnoni and Groppo, 2006; Van Gosen, 2007; Giacomini *et al.*, 2010; Vignaroli *et al.*, 2014; Punturo *et al.*, 2015; Lucci *et al.*, 2018), in contrast to the process of serpentinisation of mafic and ultramafic rocks (Karkanis, 1995; Ross and Nolan, 2003; Compagnoni and Groppo, 2006; Van Gosen, 2007; Hendrickx, 2009; Viti *et al.*, 2011; Gaggero *et al.*, 2013), where water activity-dependent mineralogical alteration triggers the asbestos growth in the form of chrysotile.

The proposed scenario considers that fibrous mineralisation in metagabbro is favoured by positive feedbacks between polyphase deformation, decompression/cooling, and fluid circulation. At both ductile and semi-brittle deformation conditions, the structurally controlled growth of fibrous amphibole is determined by the dynamic crystallisation of fibres oriented parallel to the direction of the maximum stretching, i.e. along the C-type shears in mylonitic foliation and parallel to the vein opening direction, respectively. It is noteworthy that, although the mylonitic foliation is widespread and diffuse throughout the rock volume, the fibrous growth of amphibole within the C-type shear is rather scarce. Thus, a low-to-very-low percentage of fibrous growth (the ratio between the amount of the fibrous amphibole divided by the total amount of amphibole) would be expected for this structure. On the other hand, although the shear veins are localised structures within the rock volume, the fibrous growth of amphibole is rather abundant, and a high percentage of fibrous growth is expected for these structures. Indeed, our results document that the fibrils that we documented in the shear veins of Type-2 comply with both morphological (elongate particles longer than 5.0 μm , with a minimum aspect ratio of 3:1, and showing parallel or stepped sides developed during growth) and mineralogical (actinolite asbestos for the amphibole group) criteria for asbestos classification (AHERA, 1987; OSHA, 1994; WHO, 1986). Therefore, our structural dataset implies the formation of shear veins as responsible for nucleation and localisation of asbestiform amphibole, thus defining a potential hazard for the environment related to the naturally occurring asbestos. Considering (i) an average of 5-10% in volume of asbestos amphibole in plagioclase veins and (ii) a volume of the shear veins up to 1% of the outcropping metagabbro volume (that is about 0.1 km^3), we crudely estimate 10^{-4} km^3 as the amount of asbestos amphibole over the metagabbro block.

5.3 Boundary conditions inducing asbestos growth in tectonised ophiolite rocks

Overall, a list of major preconditions and key factors for the growth of asbestos minerals in tectonised ophiolite rocks can be proposed (Fig. 12):

- Tectonic environment (Te). Tectonised ophiolites show complexities in terms of superimposed structures and mineralogical assemblages (including fibrous minerals) developed under certain conditions of temperature and pressure (e.g., Trommsdorff and Evans, 1974; Evans, 2004). The local tectonic structures are therefore considered a key rock parameter for detecting and characterising the asbestos occurrence in ophiolites (Karkanas, 1995; Compagnoni and Groppo, 2006; Giacomini *et al.*, 2010; Vignaroli *et al.*, 2011; 2014; Gaggero *et al.*, 2013; Bloise *et al.*, 2017);
- Rheology (R). Tectonic structures hosting syn-kinematic growth of asbestos mineralisation develop in both ductile (mylonitic foliation) and brittle (vein-array) rheological conditions (Vignaroli *et al.*, 2011, and references therein);
- Shear deformation (Sd). In both ductile and (semi-)brittle regimes, the concomitance of strain and dynamic recrystallisation induces minerals to become fibrous in their growth direction. In particular, asbestos formation is triggered by slickenfibre-like dynamic growth along surfaces of maximum shear deformation in mylonitic foliation and by synthaxial growth in shear veins. Conversely, static growth, such as that leading to corona structures around porphyroclasts, can explain the occurrence of non-fibrous mineralisations;
- Micro-scale textural heritages (Th). In a ductile regime, asbestos can become localised at micro-sites where mylonitic shearing overprints a former, coarse-grained and anhydrous fabric, for which an enhanced physico-chemical reworking is required. In shear veins in a more brittle regime, asbestos is localised and concentrated at micro-sites where pristine textures are occasionally oriented parallel to the dominant strain direction (e.g., the relict clinopyroxene cleavage is oriented parallel to the vein opening direction);
- Fluid circulation (Fc). Fluid-assisted crystallisation of asbestos is required within the developing shearing structures. This is attested by: (i) the syn-metamorphic amphibole growth on the early anhydrous mineralogical assemblage (i.e., the igneous clinopyroxene+plagioclase assemblage for a gabbro) in a ductile regime; and (ii) the cyclic mechanism of overpressure/mineral sealing within shear veins in a brittle regime.

We therefore consider the asbestos growth in tectonised ophiolite rocks in terms of the rock's evolving fabric (Sd-R-Th-Fc rhomb in Fig. 12), which encompasses a wide spectrum of micro- and macro-structures resulting from the superimposition of chronologically distinct tectonic

events (Te vertex in Fig. 12). The interplay between ductile and brittle structures induces secondary permeability (Sd-R-Te triangle in Fig. 12) and strain localisation (Th-R-Te triangle in Fig. 12) in the ophiolitic rock volume, which favours the processes of focussed fluid migration (Fc-Sd-Te triangle in Fig. 12) and fluid/rock interaction (Fc-Th-Te triangle in Fig. 12).

5.4 From the tectono-metamorphic history to the asbestos hazard in ophiolitic rocks

Vignaroli *et al.* (2011) proposed a qualitative parametrisation of the asbestos hazard in ophiolitic rocks as the product of geological characteristics, including the fabric heterogeneities, in response to the different tectonic/geodynamic settings. The tectono-metamorphic reworking of ophiolites in orogenic settings (Dewey and Bird, 1970; Cloos and Shreve, 1988; Cawood *et al.*, 2009) is proposed as an ideal scenario where framing the above-mentioned key factors for fibrous and, possibly, asbestos concentration in rock fabric systematics.

During the subduction-exhumation cycle Fig. 13), ophiolites undergo superimposition of chronologically distinct tectono-metamorphic events of fluid-assisted deformation and metamorphic conditions (Pressure-Temperature paths), which lead to modifications of the original stratigraphic sequence, texture, mineralogy, and rheology (Trommsdorff and Evans, 1974; Evans, 1977; Hoogerduijn Strating and Vissers, 1994; Hermann *et al.*, 2000; Dilek and Furnes, 2011). It results in a polyphase rock fabric made of superimposed deformation structures developed at ductile and at more brittle conditions. Within the wide range of deformation structures, both mylonitic shear zones and veins (numbers (1) and (2) in Fig. 13, respectively) are typical structures able to focus metamorphic reactions and newly formed mineral assemblages (e.g., Vernon, 2004; Passchier and Trouw, 2005; Austrheim, 2013). While mylonitic shearing enhances dynamic fibrous growth along shear surfaces in ductile conditions, hybrid mode opening of syntaxial veins represents possible deformation mechanism for localised asbestos crystallisation within the vein-filling material in tectonised ophiolites.

Summing up, the occurrence of asbestiform mineralisation in ophiolite rocks and the consequent open-air asbestos hazard strictly depend on (i) the rock fabric heterogeneity provided by interference and superimposition between different tectonic structures, and (ii) the dynamic crystallisation of fibrous minerals within the rock space assisted by fluid-assisted deformation. Some geometrical parameters are crucial for defining the 3D distribution of the fibrous potentially-hazardous minerals. They are (i) their spatial arrangement (mylonitic foliation can be pervasive within the rock mass, whereas veins are localised and discrete), (ii) their thickness (mylonitic foliation can be cm to m, whereas veins are in the order of mm to m), and (iii) their persistence

(mylonitic foliation can be up to kilometres, whereas veins are up to a few metres). The evaluation and quantification of parameters controlling the fibrous mineralisation may represent a starting point toward a scientifically based approach in linking the rocks properties (the natural source) to the amount of airborne asbestos (the induced product). Indexing the asbestos hazard in terms of the rock properties can contribute to determine protocols and specific techniques for supporting engineering activities in urban settings where management of asbestos-bearing rocks can induce environmental risks both for workers and for residents. Structural-based information can be used to optimise specific rock treatments based on the occurrence and the spatial distribution of those geological structures most likely to contain asbestos.

6. Conclusions

The major novelty of this work is the documentation of deformation structures, mechanisms, and boundary conditions for fibre formation and related asbestos hazard in non-serpentinised rocks that are part of tectonised ophiolites involved in orogenic construction. The main conclusions can be derived from this study are as follows:

- (1) The shear fabric development, localisation of deformation, and occurrence of inherited textures play a primary controlling role in the nucleation and development of amphibole fibres in the transition from a ductile- to a brittle-dominated deformation environment in non-serpentinised rocks.
- (2) Within the wide range of deformation structures, shear veins can create the main structural setting for asbestos concentration in non-serpentinised rocks.
- (3) In addition to the process of serpentinisation for mafic and ultramafic rocks, the dynamic crystallisation of fibrous minerals in non-serpentinised rocks defines a key process of asbestos accumulation in tectono-metamorphic ophiolites.
- (4) Boundary conditions for structures development (tectonic environment, inherited textures, rheology, kinematics, and fluid-rock interaction) and occurrence (spatial distribution and geometry) are key elements for characterising the ophiolitic rock masses in terms of factual occurrence of asbestos.
- (5) The structural approach to the analysis of fibrous minerals, as proposed in this study, should guide a multidisciplinary and multiscale research approach toward the definition of a new investigation procedure for evaluating and, possibly, forecasting the natural occurrence and hazard of asbestos in terms of rock fabric systematics.

Acknowledgments

The authors are grateful to quarry workers for providing us any logistic assistance and for stimulating discussions. This manuscript benefitted from criticisms and suggestions by the Subject Editor, Karel Schulmann, and three anonymous reviewers, who are warmly thanked.

ACCEPTED MANUSCRIPT

References

- AHERA (Asbestos Hazardous Emergency Response Act), 1987. Interim transmission electron microscopy analytical methods - mandatory and non-mandatory - and mandatory section to determine completion of response. *Federal Register*, **52**, 41857-41897, October 30.
- Andreani, M., Baronnet, A., Boullier, A.M. and Gratier J.P. 2004. A microstructural study of a “crack-seal” type serpentine vein using SEM and TEM techniques. *European Journal of Mineralogy*, **16**, 585–595.
- Andreani, M., Boullier, A.M. and Gratier, J.P. 2005. Development of schistosity by dissolution-crystallization in a Californian serpentinite gouge. *Journal of Structural Geology*, **27**, 2256–2267.
- Andreani, M., Mével, C., Boullier, A.M. and Escartín, J. 2007. Dynamic control on serpentine crystallization in veins: Constraints on hydration processes in oceanic peridotites. *Geochemistry Geophysics Geosystems*, **8**, Q02012, doi:10.1029/2006GC001373.
- ASTM D7712-11, 2011. Standard Terminology for Sampling and Analysis of Asbestos, ASTM International, West Conshohocken, PA. www.astm.org, DOI:10.1520/D7712-11.
- Austrheim, H. 2013. Fluid and deformation induced metamorphic processes around Moho beneath continent collision zones: Examples from the exposed root zone of the Caledonian mountain belt, W-Norway. *Tectonophysics*, **609**, 620-635, <https://doi.org/10.1016/j.tecto.2013.08.030>.
- Auzende, A.L., Guillot, S., Devouard, B. and Baronnet, A. 2006. Serpentinites in an Alpine convergent setting: effects of metamorphic grade and deformation on microstructures. *European Journal of Mineralogy*, **18**, 21–33.
- Barker, S.L.L., Cox, S.F., Eggins, S.M., and Gagan, M.K. 2006. Microchemical evidence for episodic growth of antitaxial veins during fracture-controlled fluid flow. *Earth and Planetary Science Letters*, **250**, 331–344.
- Bellot, J.P. 2008. Natural deformation related to serpentinisation of an ultramafic inclusion within a continental shear zone: The key role of fluids. *Tectonophysics*, **449**, 133–144.
- Bloise, A., Catalano, M., Critelli, T., Apollaro, C. and Miriello, D. 2017. Naturally occurring asbestos: potential for human exposure, San Severino Lucano (Basilicata, Southern Italy). *Environmental Earth Sciences*, **76:648**, doi:10.1007/s12665-017-6995-9.
- Bons, P.D., Elburg, M.A. and Gomez-Rivas, E. 2012. A review of the formation of tectonic veins and their microstructures. *Journal of Structural Geology*, **43**, 33-62.
- Boschi, C., Früh-Green, G.L. and Escartín, J. 2006. Occurrence and significance of serpentinite-hosted, talc- and amphibole-rich fault rocks in modern oceanic settings and ophiolite complexes: an overview. *Ophioliti*, **31**, 129–140.
- Bucher, K. and Grapes, R. 2011. *Petrogenesis of Metamorphic Rocks*. Springer-Verlag Berlin Heidelberg, 441 pp., doi 10.1007/978-3-540-74169-5.
- Cannaò, E., Scambelluri, M., Agostini, S., Tonarini, S., and Godard, M. 2016. Linking serpentinite geochemistry with tectonic evolution at the subduction plate-interface: The Voltri Massif case study (Ligurian Western Alps, Italy). *Geochimica et Cosmochimica Acta*, **190**, 115-133, doi.org/10.1016/j.gca.2016.06.034.
- Capponi, G. and Crispini, L. 2002. Structural and metamorphic signature of alpine tectonics in the Voltri Massif (Ligurian Alps, North-Western Italy). *Eclogae Geologicae Helvetiae*, **95**, 31–42.
- Capponi, G. and Crispini, L. 2006. Elemento 213–3 “Pegli”, scala 1/250000, Progetto CARG—Regione Liguria. <http://www.cartografia.regione.liguria.it>. Accessed July 2012.
- Cawood, P.A., Kröner, A., Collins, W.J., Kusky, T.M., Mooney, W.D. and Windley, B.F. 2009. Accretionary orogens through Earth history. In: Cawood, P.A. and Kröner, A. (eds.) *Earth Accretionary Systems in Space and Time*. Geological Society, London, Special Publication, **318**, 1–36.
- Chiesa, S., Cortesogno, L., Forcella, F., Galli, M., Messiga, B., Pasquarè, G., Pedemonte, G.M., Piccardo, G.B., and Rossi, P.M. 1975. Assetto strutturale ed interpretazione geodinamica del Gruppo di Voltri. *Bollettino della Società Geologica Italiana*, **94**, 555–581.
- Clinkenbeard, J.P., Churchill, R.K. and Lee, K. 2002. *Guidelines for geologic investigations of naturally occurring asbestos in California*. Special Publication **124**. Department of Conservation, California Geological Survey.
- Coleman, R.G. 1977. *Ophiolites: ancient oceanic lithosphere?* Berlin: Springer-Verlag.

- Compagnoni, R. and Groppo, C. 2006. Gli amianti in Val di Susa e le rocce che li contengono. *Rendiconti della Società Geologica Italiana*, **3**, 21–28.
- Cox, S.F. 2010. The application of failure mode diagrams for exploring the roles of fluid pressure and stress states in controlling styles of fracture-controlled permeability enhancement in faults and shear zones. *Geofluids*, **10**, 217–233, doi: 10.1111/j.1468-8123.2010.00281.x.
- Cox, S.F. and Etheridge, M.A. 1983. Crack-seal fibre growth mechanisms and their significance in the development of oriented layer silicate microstructures. *Tectonophysics*, **92**, 147–170.
- Cox, S.F., Knackstedt, M.A. and Braun, J. 2001. Principles of structural control and permeability and fluid flow in hydrothermal systems. *Reviews of Society of Economic Geologists*, **14**, 1–24.
- Crispini, L., Federico, L., Capponi, G. and Spagnolo, C. 2009. Late orogenic transpressional tectonics in the “Ligurian Knot”. *Bollettino della Società Geologica Italiana*, **128** (2), 433–441.
- Crispini, L. and Frezzotti, M.L. 1998. Fluid inclusion evidence for progressive folding during decompression in metasediments of the Voltri Group (Western Alps, Italy). *Journal of Structural Geology*, **20**, 1733–1746.
- Davis, G.H., Reynolds, S.J. and Kluth, C. 2011. *Structural geology of rocks and regions*, 3rd ed. John Wiley & Sons, Inc., U.S.A., 861 pp.
- Dilek, Y and Furnes, H. 2011. Ophiolite genesis and global tectonics: Geochemical and tectonic fingerprinting of ancient oceanic lithosphere. *Geological Society of America Bulletin*, **123**, 387–411, doi: 10.1130/B30446.1
- Dorling M and Zussman J., 1987. Characteristics of asbestiform and non-asbestiform calcic amphiboles. *Lithos*, **20**, 469–489.
- Evans, B.W. 1977. Metamorphism of alpine peridotites and serpentinites. *Annual Review of Earth and Planetary Sciences*, **5**, 397–448.
- Evans, B.W., 2004. The Serpentine Multisystem Revisited: Chrysotile is metastable. *International Geology Review*, **46**, 479–506, 2004.
- Federico, L., Crispini, L., Scambelluri, M. and Capponi, G. 2007a. Ophiolite mélange zone records exhumation in a fossil subduction channel. *Geology*, **35**, 499–502.
- Federico, L., Crispini, L., Scambelluri, M. and Capponi, G. 2007b. Different PT paths recorded in a tectonic mélange (Voltri Massif, NW Italy): Implications for the exhumation of HP rocks. *Geodinamica Acta*, **20**, 3–19, doi:10.3166/ga.20.3-19.
- Federico, L., Spagnolo, C., Crispini, L. and Capponi G. 2009. Fault-slip analysis in the metaophiolites of the Voltri Massif: constraints for the tectonic evolution at the Alps/Apennine boundary. *Geological Journal*, **44**, 225–240.
- Gabrielse, H. 1960. The genesis of chrysotile asbestos in the Cassiar Asbestos deposit, northern British Columbia. *Economic Geology*, **55**, 327–337.
- Gaggero, L., Crispini, L., Isola, E. and Marescotti, P. 2013. Asbestos in natural and anthropic ophiolitic environments: a case study of geohazards related to the Northern Apennine ophiolites (Eastern Liguria, Italy). *Ofioliti*, **38**, 29–40.
- Giacomini, F., Boerio, V., Polattini, S., Tiepolo, M., Tribuzio, R. and Zanetti, A. 2010. Evaluating asbestos fibre concentration in metaophiolites: a case study from the Voltri Massif and Sestri-Voltaggio Zone (Liguria, NW Italy). *Environmental Earth Sciences*, **61**, 1621–1639, doi:10.1007/s12665-010-0475-9.
- Gianfagna, A., Ballirano, P., Bellatreccia, F., Bruni, B., Paoletti, L. and Oberti, R. 2003. Characterization of amphibole fibres linked to mesothelioma in the area of Biancavilla, Eastern Sicily, Italy. *Mineralogical Magazine*, **67**(6), 1221–1229, doi: 10.1180/0026461036760160.
- Groppo, C. and Compagnoni, R. 2007. Ubiquitous fibrous antigorite veins from the Lanzo Ultramafic Massif, Internal Western Alps (Italy): characterisation and genetic conditions. *Periodico di Mineralogia*, **76**, 169–181.
- Gunter, M.E., Belluso, E. and Mottana, A. 2007. Amphiboles: environmental and health concerns. *Reviews in Mineralogy and Geochemistry*, **67**, 453–516.
- Hancock, P.L. 1985. Brittle microtectonics: principles and practice. *Journal of Structural Geology*, **7**, 437–457.
- Health and Safety Executive, 1997. *Dust: general principles of protection*. Health and safety executive, Sudbury, p 44.

- Hendrickx, M. 2009. Naturally occurring asbestos in eastern Australia: a review of geological occurrence, disturbance and mesothelioma risk. *Environmental Geology*, **57**, 909–926
- Hermann, J., Müntener, O. and Scambelluri, M. 2000. The importance of serpentinite mylonites for subduction and exhumation of oceanic crust. *Tectonophysics*, **327**, 225–238.
- Hirauchi, K.I. and Yamaguchi, H. 2007. Unique deformation processes involving the recrystallization of chrysotile within serpentinite: implications for aseismic slip events within subduction zones. *Terra Nova*, **19**, 454–461.
- Hirose, T., Bystricky, M., Kunze, K. and Stünitz, H. 2006. Semi-brittle flow during dehydration of lizardite–chrysotile serpentinite deformed in torsion: Implications for the rheology of oceanic lithosphere. *Earth and Planetary Science Letters*, **249**, 484–493.
- Hoogerduijn Strating, E.H. 1994. Extensional faulting in an intraoceanic subduction complex—Working hypothesis for the Palaeogene of the Alps - Apennine system. *Tectonophysics*, **238**, 255–273, doi:10.1016/0040-1951(94)90059-0.
- Hoogerduijn Strating, E.H. and Vissers, R.L.M. 1994. Structures in natural serpentinite gouges. *Journal of Structural Geology*, **16**, 1205–1215
- IARC (International Agency for Research on Cancer) 1987. *Monographs on the evaluation of the carcinogenic risk to humans. Overall evaluations of carcinogenicity: an updating of IARC Monographs*, **1-42**, Suppl 7. WHO-IARC, France, pp 106–116.
- IARC (International Agency for Research on Cancer) 2012. *Monographs on the evaluation of the carcinogenic risk to humans. Arsenic, metals, fibres, and dusts*. IARC Monographs, **100**. World Health Organization, pp 11–465.
- Karkanis, P. 1995. The slip-fiber chrysotile asbestos deposit in the Zidani area, northern Greece. *Ore Geology Reviews*, **10**, 19–29.
- Leake, B.E., Wooley, A.R., Birch, W.D., Burke, E.A.J., Ferraris, G., Grice, J.D., Hawthorne, F.C., Kisch, H.J., Krivovichev, V.G., Schumacher, J.C., Stephenson, N.C.N., and Whittaker, E.J.W. 2004. Nomenclature of amphiboles: additions and revisions to the International Mineralogical Association's amphibole nomenclature. *American Mineralogy*, **89**, 883–887.
- Lee, R.J., Strohmeier, B.R., Bunker, K.L. and Van Orden, D.R. 2008. Naturally occurring asbestos - A recurring public policy challenge. *Journal of Hazardous Materials*, **153**, 1–21.
- Li, X.P., Rahn, M. and Bucher, K. 2004. Serpentinities of the Zermatt-Saas ophiolite complex and their texture evolution. *Journal of Metamorphic Geology*, **22**, 159–177.
- Lucci, F., Della Ventura, G., Conte, A., Nazzari, M., and Scarlato, P. 2018. Naturally Occurring Asbestos (NOA) in granitoid rocks, a case study from Sardinia (Italy). *Minerals*, **8**, 442; doi:10.3390/min8100442.
- Malatesta, C., Crispini, L., Federico, L., Capponi, G., Scambelluri, M. 2012. The exhumation of high pressure ophiolites (Voltri Massif, Western Alps): Insights from structural and petrologic data on metagabbro bodies. *Tectonophysics*, **568–569**, 102–123, doi:10.1016/j.tecto.2011.08.024.
- Messiga, B. and Scambelluri, M. 1991. Retrograde P–T–t path for the Voltri Massif eclogites (Ligurian Alps, Italy): some tectonic implications. *Journal of Metamorphic Geology*, **9**, 93–109.
- Moody, J.B., 1976. Serpentinization: a review. *Lithos*, **9**, 125–138.
- National Institute for Occupational Safety and Health (NIOSH), 2011. *Asbestos fibers and other elongate mineral particles: state of the science and roadmap for research*. DHHS Publication No. 2011-159.
- Norrell G.T., Teixell A., Harper G.D., 1989. Microstructure of serpentinite mylonites from the Josephine ophiolite and serpentinitization in retrogressive shear zones, California. *Geological Society of America Bulletin*, **101**;673–682, doi: 10.1130/0016-7606.
- OSHA (Occupational Safety and Health Administration), 1994. Rules and Regulations, Department of Labor: 29 CFR 657 Parts 1910, 1915 and 1926, 59 FR 40964, RIN: 1218-AB25; Occupational Exposure to Asbestos; August 1994-658 Final Rule; Appendix B of 1910.1001; 1. Introduction.
- O'Hanley D.S., 1996. *Serpentinities—Records of tectonic and petrological history*. Oxford University Press, New York.
- Otsuki, M. and Banno, S. 1990. Prograde and retrograde metamorphism of hematite-bearing basic schists in the Sanbagawa belt in central Shikok. *Journal of Metamorphic Geology*, **8**, 425–439.

- Pan, X.L., Day, H.W., Wang, W., Beckett, L.A. and Schenker, M.B. 2005. Residential proximity to naturally occurring asbestos and mesothelioma risk in California. *American Journal of Respiratory and Critical Care Medicine*, **172**, 1019–1025.
- Passchier, C.W. and Trouw, R.A.J. 2005. *Microtectonics*. Berlin: Springer.
- Piccardo, G.B. 2012. Subduction of a fossil slow–ultraslow spreading ocean: a petrology constrained geodynamic model based on the Voltri Massif, Ligurian Alps, Northwest Italy. *International Geology Review*, DOI:10.1080/00206814.2012.746806.
- Phillips, F.C. 1927. The serpentines and associated rocks and minerals of the Shetland Islands. *Quarterly Journal of the Geological Society*, **83**, 622–652, doi:10.1144/GSL.JGS.1927.083.01-05.26.
- Punturo, R., Bloise, A., Critelli, T., Catalano, M., Fazio, E. and Apollaro, C. 2015. Environmental implications related to Natural Asbestos Occurrences in the ophiolites of the Gimigliano-Mount Reventino Unit (Calabria, Southern Italy). *International Journal of Environmental Research*, **9**(2), 405–418.
- Ramsey, J.M. and Chester, F.M. 2004. Hybrid fracture and the transition from extension fracture to shear fracture. *Nature*, **428**, 63–66.
- Reinen, L.A. 2000. Seismic and aseismic slip indicators in serpentinite gouge. *Geology*, **28**, 135–138.
- Rohl, A.N., Langer, A.M., and Selikoff I.R. 1977. Environmental asbestos pollution related to use of quarried serpentinite rock. *Science*, **196**, 1319–1322.
- Ross, M., Kuntze, R.A. and Clifton, R.A. 1984. A definition for asbestos. In: B. Levadie (ed.) *Definitions for asbestos and other health-related silicates, ASTM STP 834*. Philadelphia: American Society for Testing and Materials, 139–147.
- Ross, M. and Nolan, R.P. 2003. History of asbestos discovery and use and asbestos-related disease in context with the occurrence of asbestos within ophiolite complexes. *Geological Society of America Special paper*, **373**, 447–470.
- Scambelluri, M., Hoogerduijn Strating, E.H., Piccardo, G.B., Vissers, R.L.M. and Rampone, E. 1991. Alpine olivine- and titanite-clinohumite-bearing assemblages in the Erro-Tobbio peridotite (Voltri Massif, NW Italy). *Journal of Metamorphic Geology*, **9**, 79–91.
- Shelley, D. 1994. Spider texture and amphibole preferred orientations. *Journal of Structural Geology*, **16**, 709–717.
- Sibson, R.H. 2004. Controls on maximum fluid overpressure defining conditions for mesozonal mineralisation. *Journal of Structural Geology*, **26**, 1127–1136.
- Strohmeier, B.R., Huntington, J.C., Bunker, K.L., Sanchez, M.S., Allison, K., Lee, R.J., 2010. What is asbestos and why is it important? Challenges of defining and characterizing asbestos. *International Geology Review*, **52**:7, 801–872, doi: 10.1080/00206811003679836.
- Taber, S. 1918. The origin of veinlets in the Silurian and Devonian strata of central New York. *Journal of Geology*, **26**, 56–73.
- Trommsdorff, V. and Evans, B.W. 1974. Alpine metamorphism of peridotitic rocks. *Schweiz. Mineral. Petrogr. Mitt.*, **54**, 333–352.
- Twiss, R.J. and Moores, E.M. 2007. *Structural geology*. W. H. Freeman And Company, New York (U.S.A.), 742 pp.
- Van Gosen, B.S. 2007. The geology of asbestos in the United States and its practical applications. *Environmental & Engineering Geoscience*, **13**, 55–68.
- Vanossi, M., Cortesogno, L., Galbiati, B., Messiga, B., Piccardo, G., Vannucci, R., 1984. Geologia delle Alpi Liguri: dati, problemi, ipotesi. *Memorie della Società Geologica Italiana*, **28**, 5–75.
- Vernon, R.H. 2004. *A practical guide to rock microstructure*. Cambridge: University Press.
- Vignaroli, G., Ballirano, P., Belardi, G. and Rossetti, F. 2014. Asbestos fibre identification vs. evaluation of asbestos hazard in ophiolitic rock mélanges, a case study from the Ligurian Alps (Italy). *Environmental Earth Sciences*, **72**, 3679–3698, doi:10.1007/S12665-014-3303-9.
- Vignaroli, G., Faccenna, C. and Rossetti, F. 2009. Retrogressive fabric development during exhumation of the Voltri Massif (Ligurian Alps, Italy): arguments for an extensional origin and implications for the Alps–Apennines linkage. *International Journal of Earth Sciences*, **98**, 1077–1093.

- Vignaroli, G., Rossetti, F., Belardi, G. and Billi, A. 2011. Linking rock fabric to fibrous mineralisation: a basic tool for the asbestos hazard. *Natural Hazards and Earth System Sciences*, **11**, 1267–1280, doi:10.5194/nhess-11-1267-2011.
- Vignaroli, G., Rossetti, F., Rubatto, D., Theye, T., Lisker, F. and Phillips, D. 2010. Pressure-temperature-deformation-time (P-T-d-t) exhumation history of the Voltri Massif HP complex, Ligurian Alps, Italy. *Tectonics*, **29**(6), doi:10.1029/2009TC002621.
- Vignaroli, G., Rossetti, F., Bouybaouene, M., Massonne, H.J., Theye, T., Faccenna, C. and Funicello, R. 2005. A counter-clockwise P–T path for the Voltri Massif eclogites (Ligurian Alps, Italy). *Journal of Metamorphic Geology*, **23**, 533–555.
- Viti, C. and Hirose, T. 2009. Dehydration reactions and micro/nanostructures in experimentally-deformed serpentinites. *Contributions to Mineralogy and Petrology*, **157**, 327–338, doi:10.1007/s00410-008-0337-6.
- Viti, C., Giacobbe, C. and Gualtieri, F., 2011. Quantitative determination of chrysotile in massive serpentinites using DTA: Implications for asbestos determinations. *American Mineralogist*, **96**, 1003–1011, doi: 10.2138/am.2011.3734 1003
- Wicks, F.J. and Wittaker, E.J.W. 1977. Serpentine textures and serpentinization. *Canadian Mineralogist*, **15**, 459–488.
- World Health Organization (WHO) 1986. *Asbestos and other natural mineral fibres*. Environmental Health Criteria, No. 53, Geneva.
- Yavuz, F. 2007. WinAmphcal: a Windows program for the IMA-04 amphibole classification. *Geochemistry, Geophysics, Geosystems*, **8**(1), doi:10.1029/2006GC001391.

Figure captions

Fig. 1 – Localisation of the study area. a) Geological sketch of the Ligurian Alps and Western Alps, Italy; b) geological–structural framework of the area surrounding the studied quarry (after Capponi and Crispini 2006); c) schematic representation of a quarried site that has been used for structural investigations on the considered metagabbro block. The most evident deformation structures are shown. Black arrows in vein pictures represent direction of vein opening, which is either orthogonal or oblique to the vein wall. [mid-width width]

Fig. 2 – Outcrops and selected samples. a) Sample TB62: fine-grained massive metagabbro; b) sample TB59: foliated metagabbro characterised by a highly-dipping syn-greenschist mylonitic foliation; c) detail of the syn-greenschist fabric composed of green amphibole+plagioclase association surrounding relicts of clinopyroxene; d) sample TB61: half-metre-spaced set of metamorphic vein affecting the foliated metagabbro; e) view of the vein surface consisting of plagioclase+quartz matrix hosting cm-width soft bundles of fibrous amphibole; f) detail of the amphibole bundles nested within coarse plagioclase grains. am: amphibole; cpx: clinopyroxene; pl: plagioclase; qtz: quartz. [mid-width width]

Fig. 3 – Thin section views of selected samples. a) Sample TB62: fine-grained massive metagabbro consisting of a composite groundmass of clinopyroxene+plagioclase; b) sample TB59: foliated metagabbro showing a syn-greenschist mylonitic foliation replacing the pristine coarse-grained magmatic fabric; c) sample TB61: plagioclase+quartz metamorphic vein. The vein interface truncates the syn-greenschist foliation, which is disposed at high angle with respect to the interface, and some magmatic relicts; d) schematic drawing of the vein opening direction that is slightly oblique to the metagabbro/vein interface. All pictures are scans of the thin sections. am: amphibole; cpx: clinopyroxene; pl: plagioclase; qtz: quartz. [mid-width width]

Fig. 4 – Petrographic details of the massive metagabbro (sample TB62). a) fine-grained groundmass of clinopyroxene+plagioclase; b) back-scattered electron (BSE) imaging shows a rounded clinopyroxene grain affected by internal microcracks and an alteration corona. Both the microcracks and the corona structure are filled by amphibole grains developed during the syn-greenschist fabric; c) X-ray maps do not show appreciable chemical zoning within the amphibole grains forming the corona. am: amphibole; chl: chlorite; cpx: clinopyroxene; pl: plagioclase. [single column width]

Fig. 5 – Petrographic details of the foliated metagabbro (sample TB59). a) Detail of the syn-greenschist fabric consisting of pervasive (sub-millimetre thick) C-type shear bands and S-foliation (see scheme in the insert); b) BSE image and (c) X-ray maps of the C-type shear bands consisting of elongate grains of amphibole in textural association with chlorite and subordinate titanite; d) a large, magmatic, clinopyroxene rimmed by an alteration corona composed of amphibole grains developed during the syn-greenschist fabric; e) the BSE and f) the X-ray maps show that the corona structure around the magmatic clinopyroxene consists of prismatic/tabular amphibole grains disposed in a randomised arrangement. Pictures a) and d) are taken under crossed polars. am: amphibole; chl: chlorite; cpx: clinopyroxene; pl: plagioclase; qtz: quartz; ttn: titanite. [mid-width width]

Fig. 6 – Petrographic details of the vein post-dating the syn-greenschist mylonitic foliation (sample TB61). a) Detail of the vein interface cutting through the metamorphic foliation. Fibrous amphibole, arranged either as isolated specimens or as fan-shaped aggregates, develops within the vein, with growth sense from the interface toward the centre of the vein (i.e., to the bottom of the micro-picture); b-c) details of the vein interface cutting through a clinopyroxene relict. Similar to the previous case, amphibole develops at the vein interface and penetrates toward the centre of the vein; d) detail of the vein interface cutting through a fine-grained domain of the metagabbro fabric. The lack of fibrous amphibole within this portion of the plagioclase+quartz vein is documented by the BSE imaging in e). Note, on the other hand, the occurrence of fibrous amphibole within intrafoliar vein. Pictures a) and c) are in natural light, whereas pictures b) and d) are at crossed polars. am: amphibole; cpx: clinopyroxene; pl: plagioclase; qtz: quartz. [mid-width width]

Fig. 7 – Petrographic details of the vein post-dating the syn-greenschist mylonitic foliation (sample TB61). a) Coarse-grained clinopyroxene truncated by the metagabbro-vein interface. Pyroxene cleavage is rather evident as well as the fibrous amphibole grown from the interface toward the centre of the vein. The vein is filled by plagioclase with a blocky texture; b) and c) the clinopyroxene is characterised by a cleavage oriented roughly perpendicular to the metagabbro-vein interface. Note the parallelism between the trend of the clinopyroxene cleavage and the trend of growing fibrous amphibole; d) and e) BSE images showing that

the site of nucleation of each fibre corresponds to cleavage-bounded microdomains of clinopyroxene; f) BSE image detailing the occurrence of amphibole as individual fibres within the plagioclase±quartz vein. Note the occurrence of very thin particles (fibrils) derived by the cleavage fragmentation of the fibres; g) BSE image detailing a micro-crack within the clinopyroxene. This crack is filled by a groundmass composed of chlorite non-fibrous amphibole, and sporadic titanite. Pictures a) and b) are taken under crossed polars, whereas picture c) is taken in natural light. am: amphibole; chl: chlorite; cpx: clinopyroxene; pl: plagioclase; qtz: quartz; ttn: titanite. [mid-width width]

Fig. 8 – Petrographic details of the vein post-dating the syn-greenschist mylonitic foliation (sample TB61). a) and b) BSE images and X-ray maps of two selected domains along the metagabbro-vein interface. X-ray maps shows that fibrous amphibole grown from the interface is not characterised by appreciable chemical zoning. [mid-width width]

Fig. 9 – Diagram classification of the analysed amphiboles (after Leake *et al.*, 2004). [single column width]

Fig. 10 – Structural-petrographic scenario of fibrous amphibole development in metagabbro including diffuse syn-greenschist overprint attained at ductile regime (Type-1) and localised shear veining attained at semi-brittle regime (Type-2). [mid-width width]

Fig. 11 – The complete failure diagram. The mylonitic foliation (Type-1 in Fig. 10) is framed within the von Mises ductile failure criterion. The veining mechanism (Type-2 in Fig. 10), conversely, is framed within the hybrid mode failure. The main role of fluid pressure (P_f) is considered to induce an extensional component to the failure. σ_n : normal stress; τ : shear stress; σ_1 and σ_3 : maximum and minimum stresses, respectively; f : internal angle of friction. [mid-width]

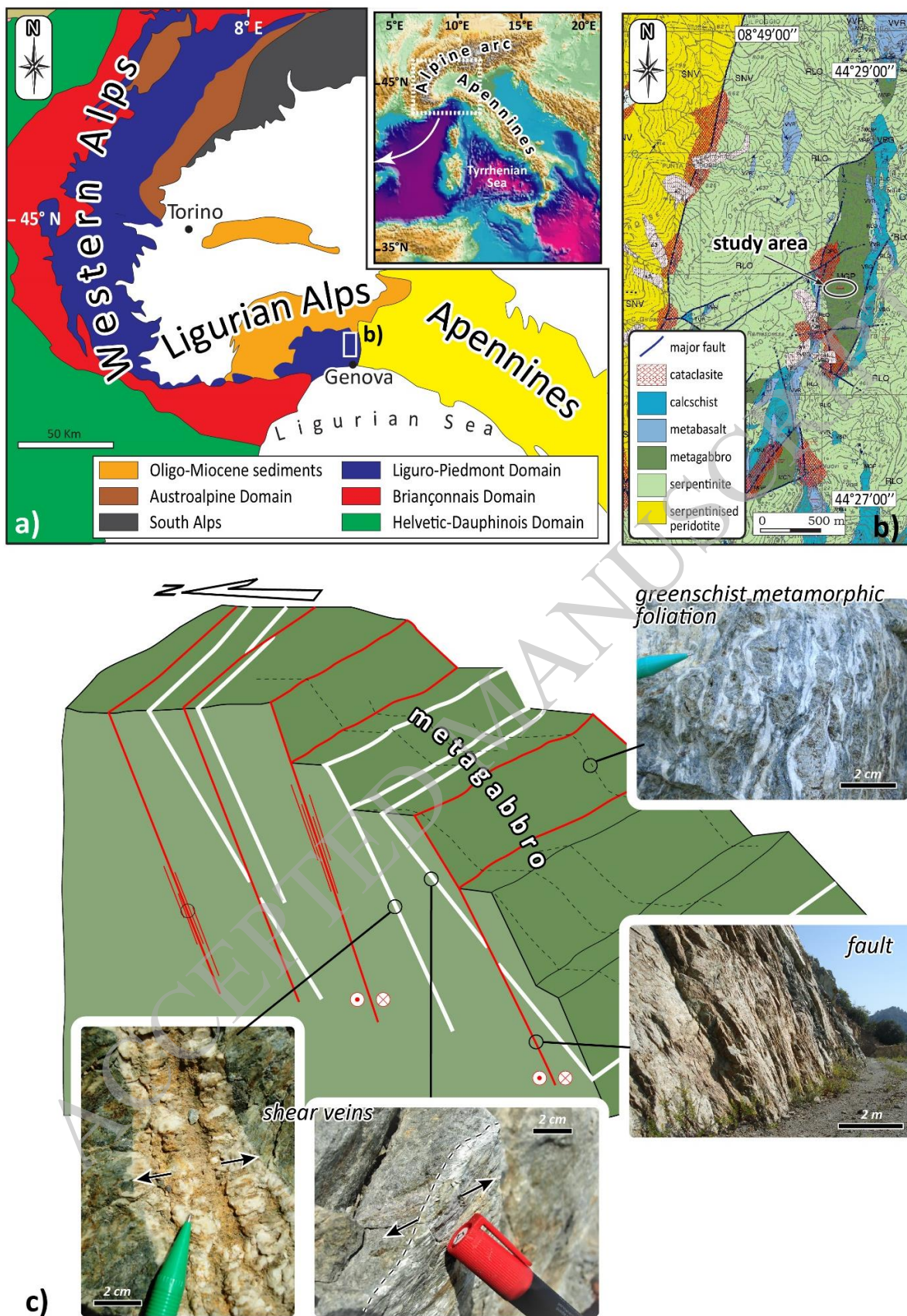
Fig. 12 – Schematic diagram illustrating structural factors, as well as their interaction and feedbacks, favouring concentration of asbestos in non-serpentinised rock following insights from this study. [mid-width]

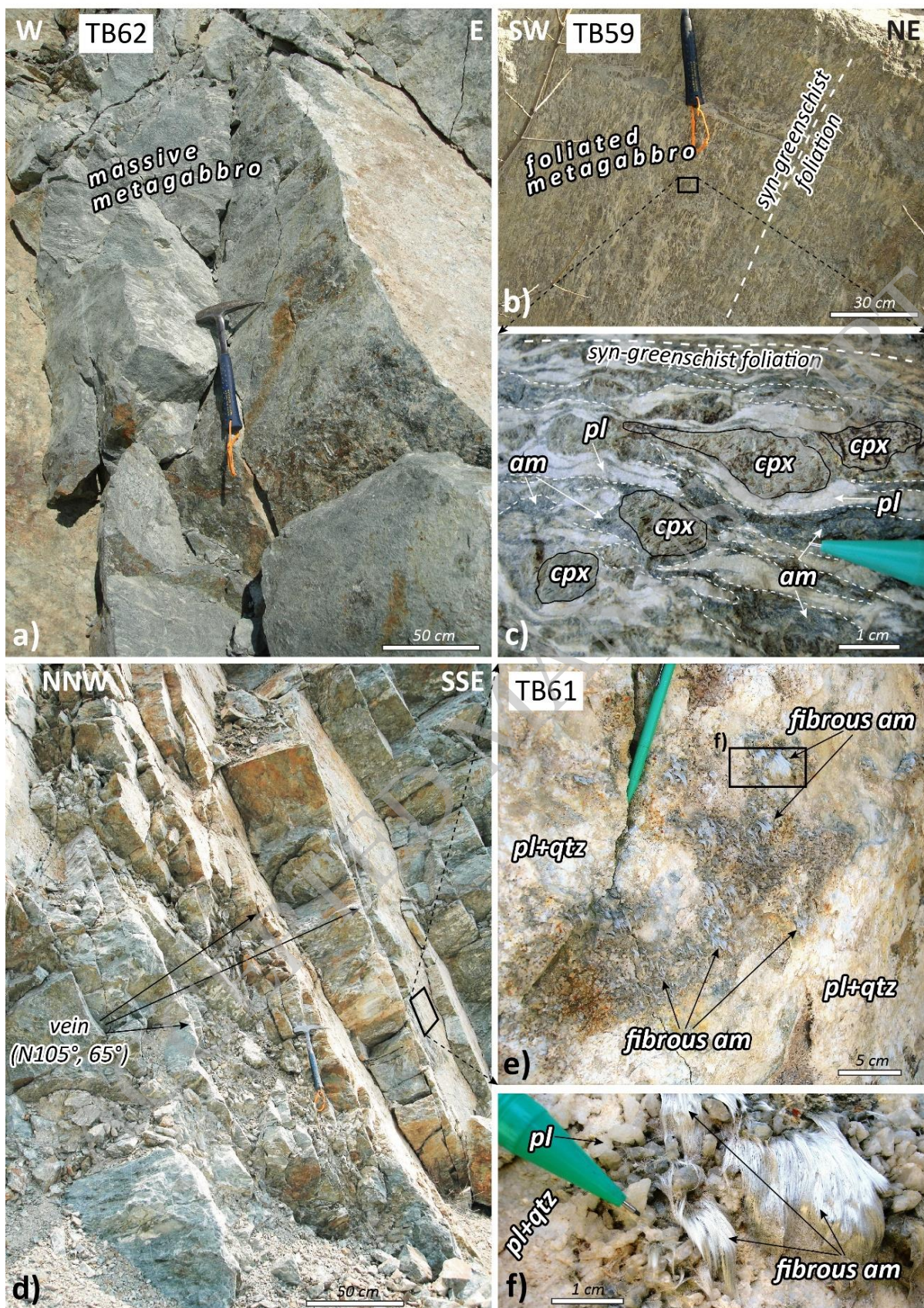
Fig. 13 – Schematic scenario of orogenic accretionary wedge used for framing deformation structures and boundary conditions leading to concentration, and possible hazard, of asbestos amphibole in ophiolitic rocks. Numbers (1) and (2) refer to representative structural and metamorphic conditions for the mylonitic greenschist fabric and the shear veining, respectively, as documented in this study. Amphiboles fields are from Otsuki and Banno (1990). Act: actinolite; Hbl: hornblende. [mid-width]

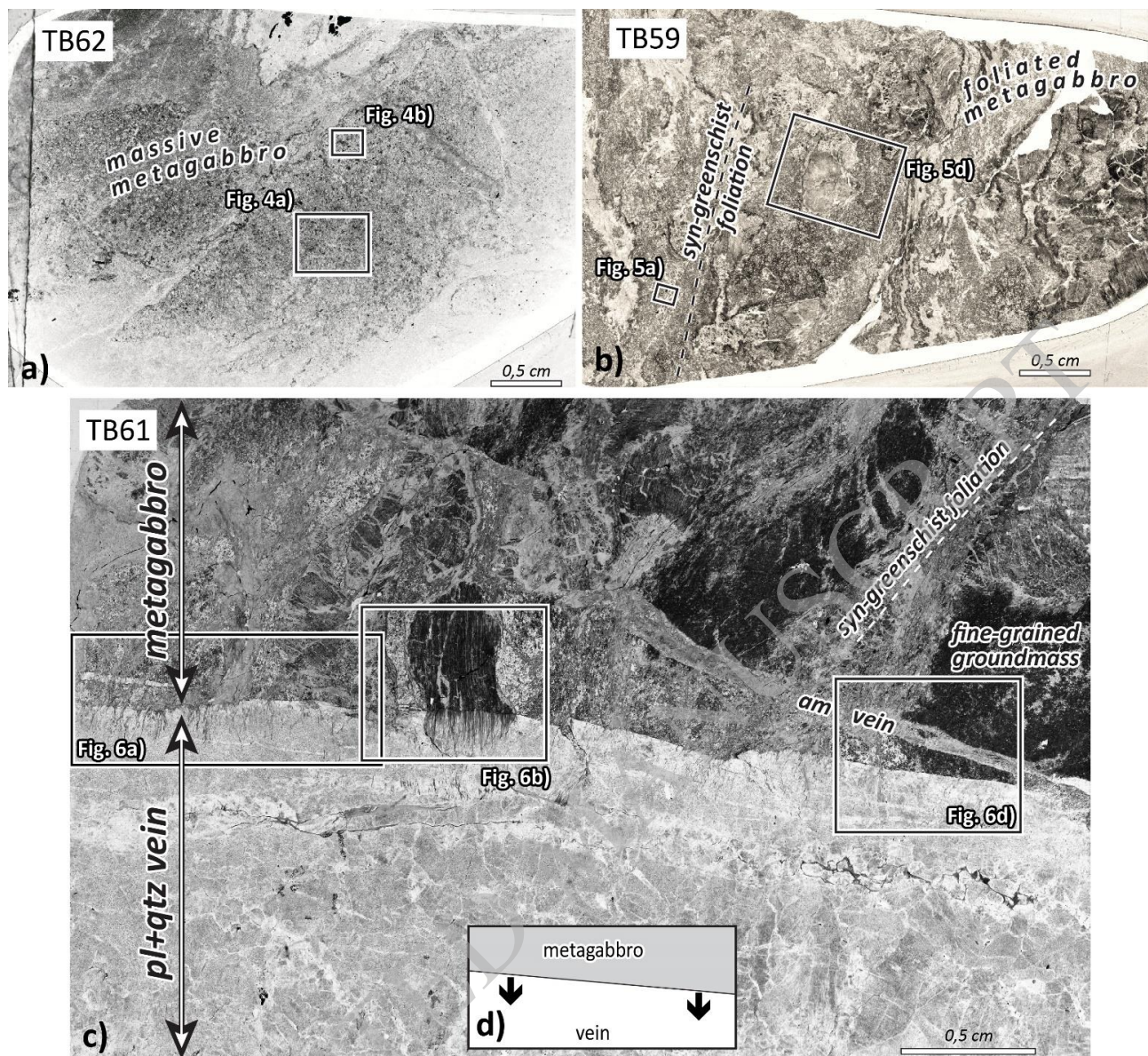
Table captions

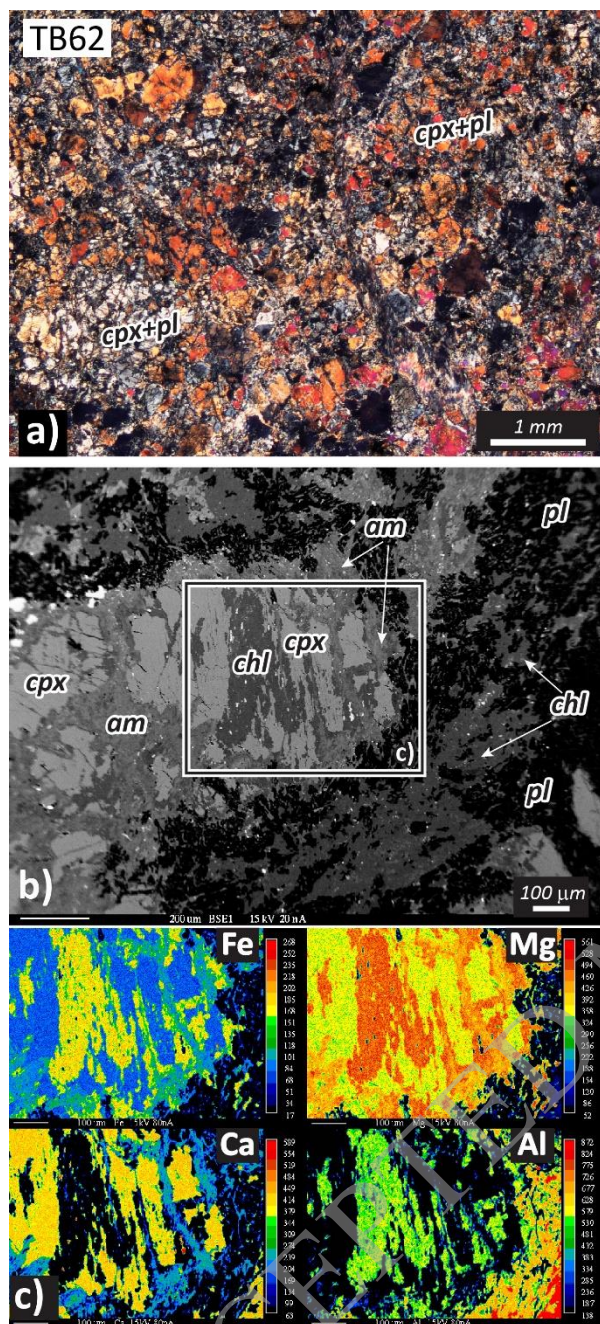
Table 1. Samples, mineral assemblages, and analytical methods.

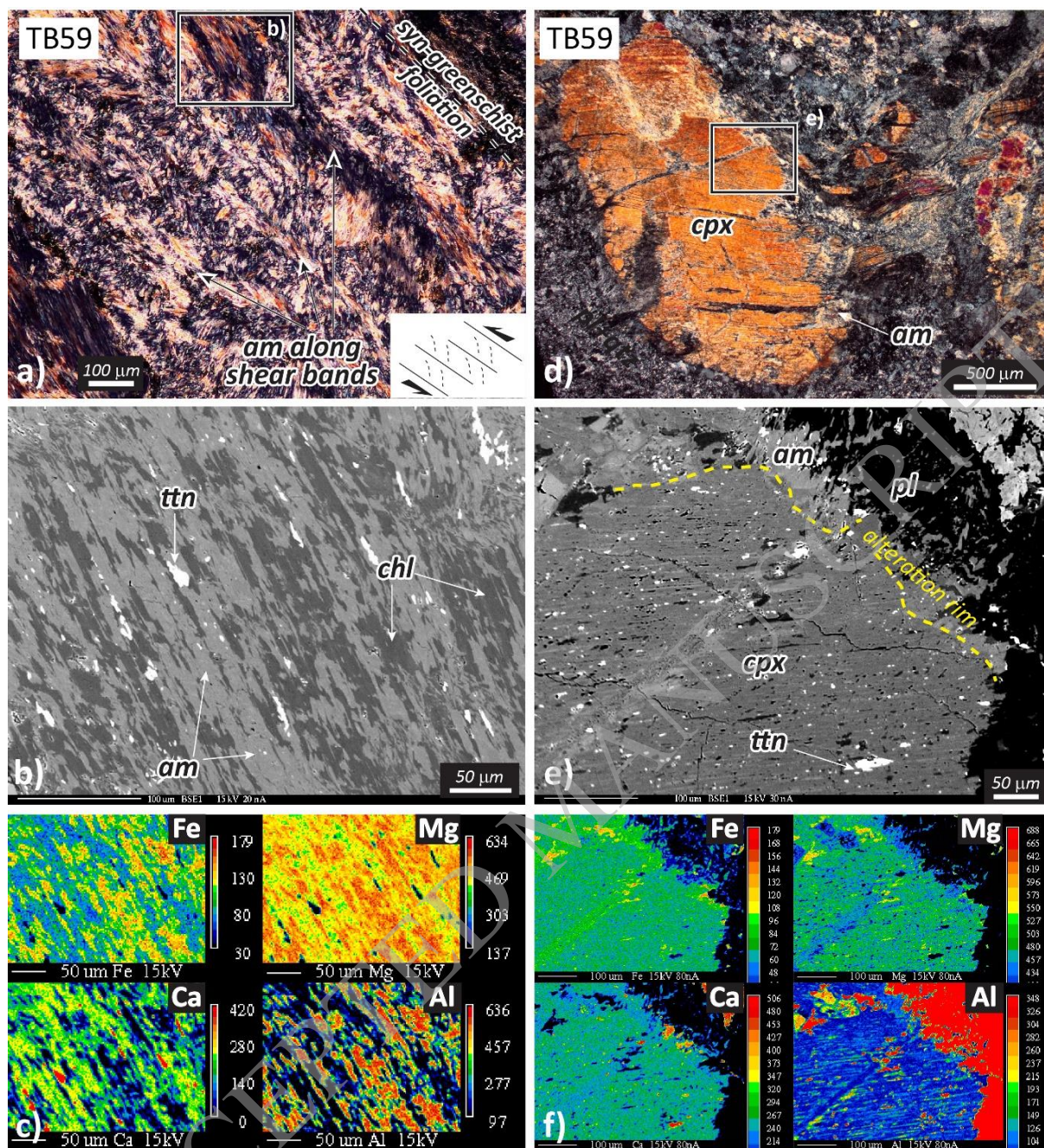
Table 2. Chemical composition of selected analysed amphiboles.

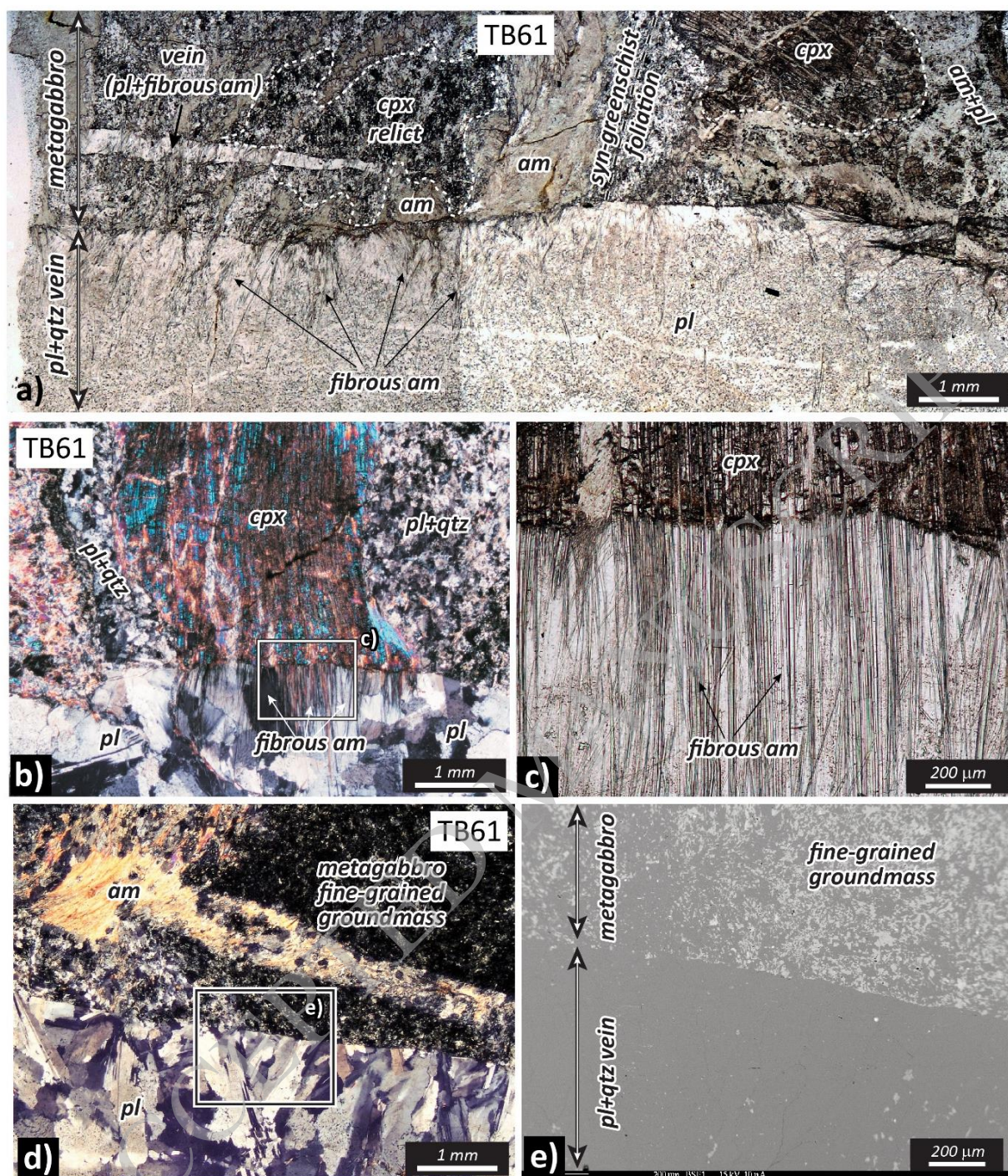


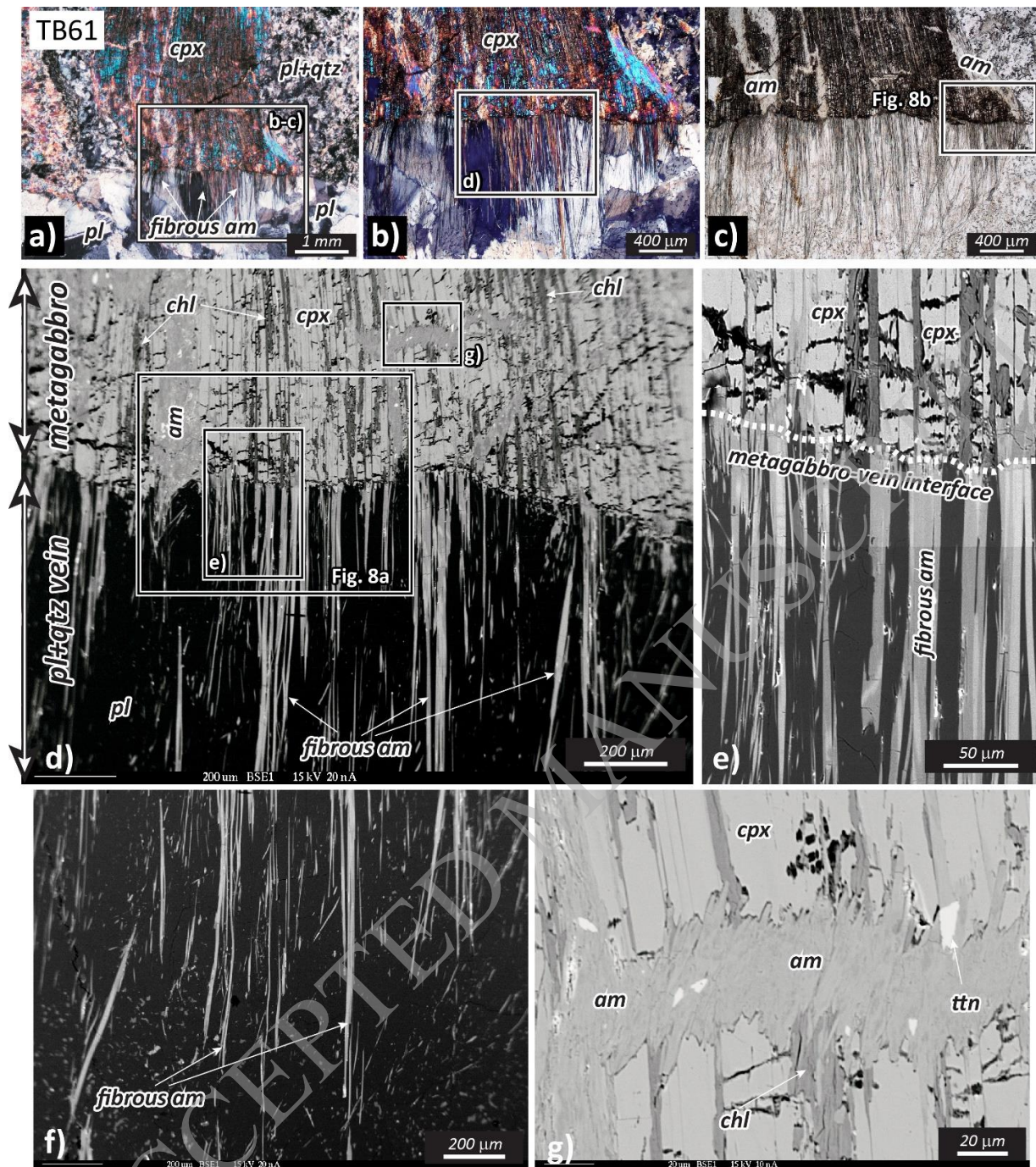


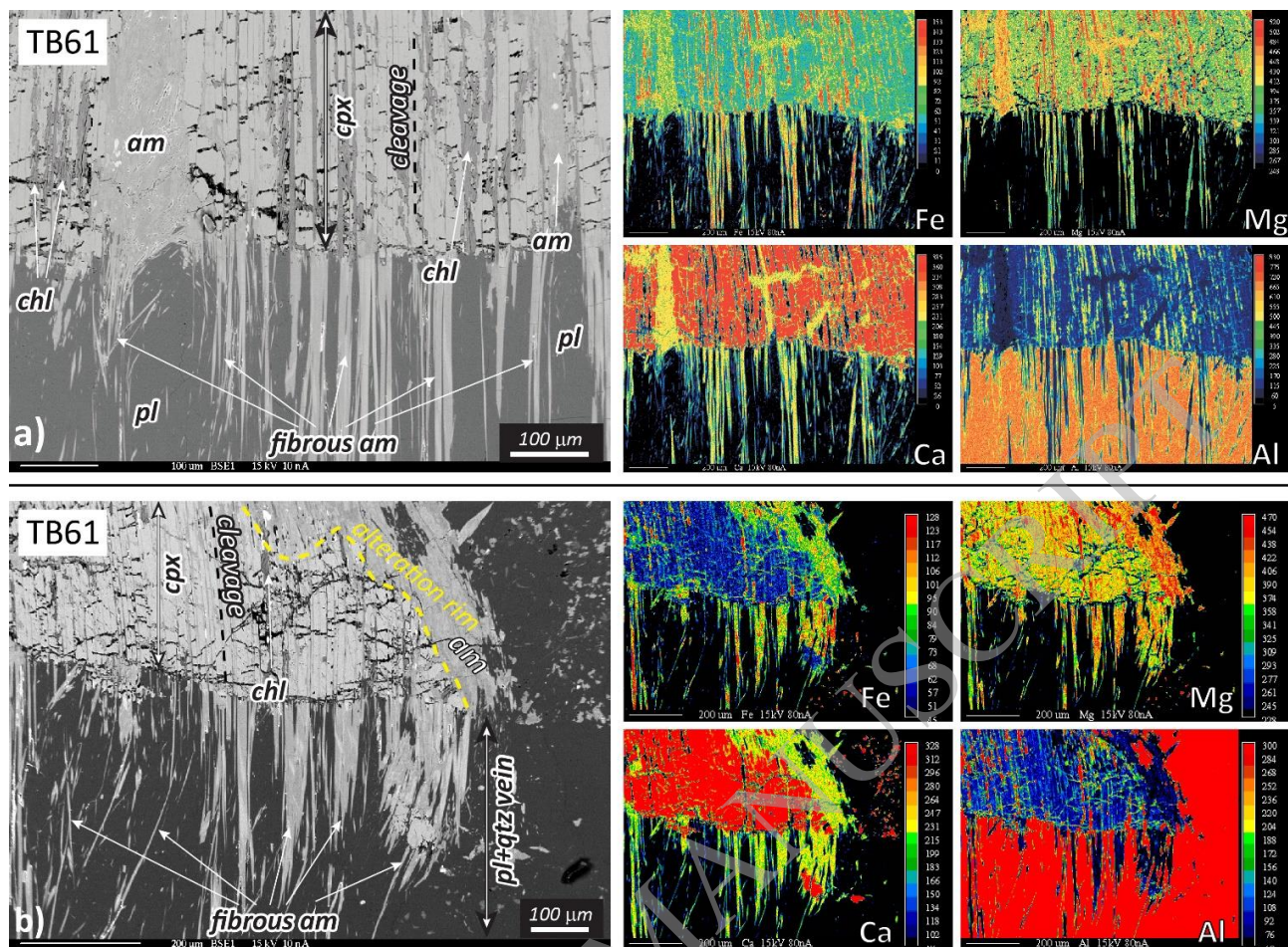


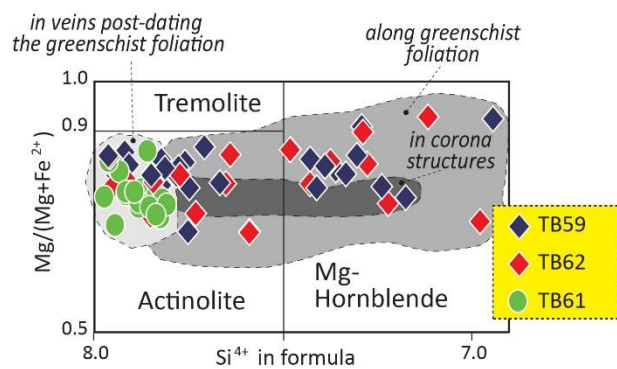


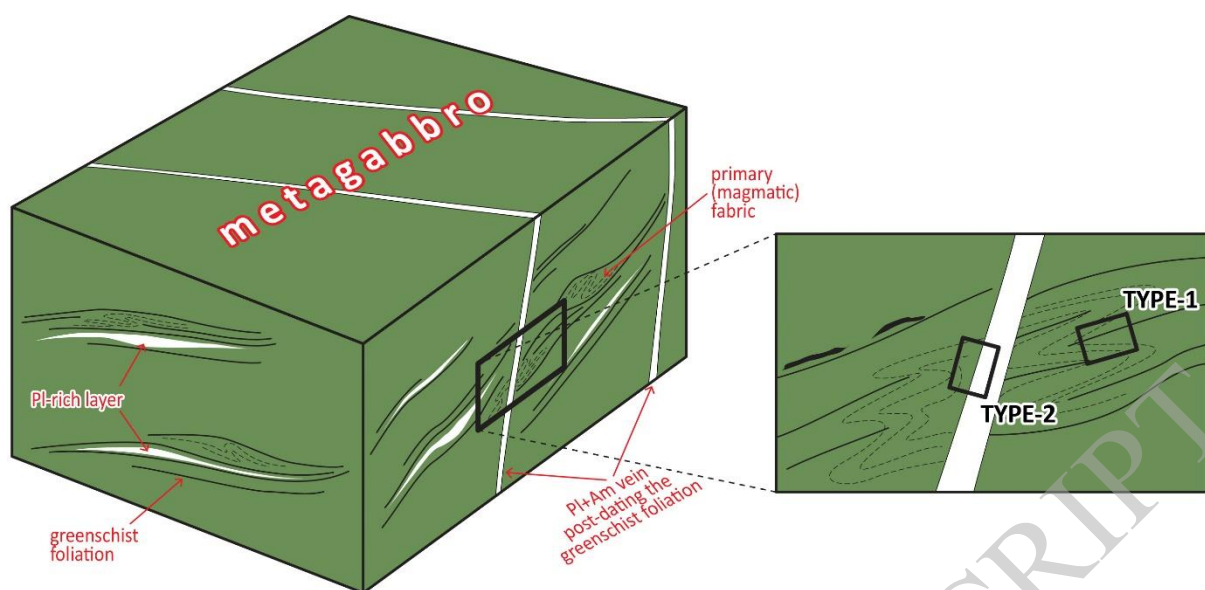




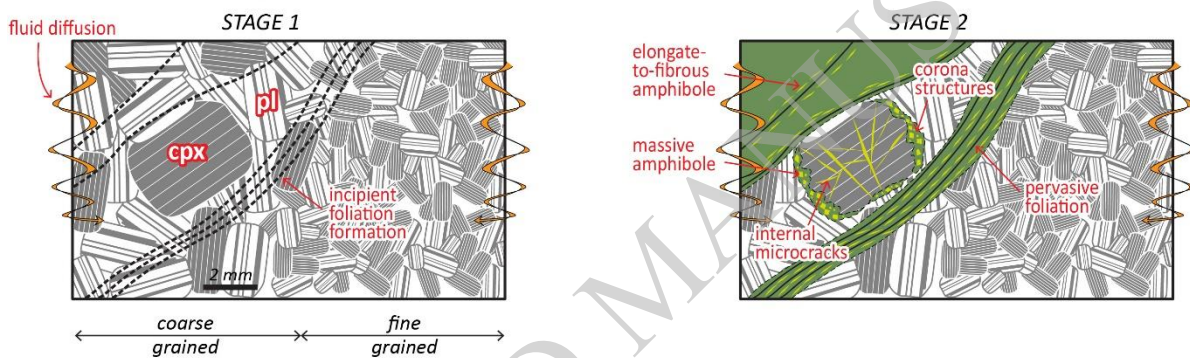




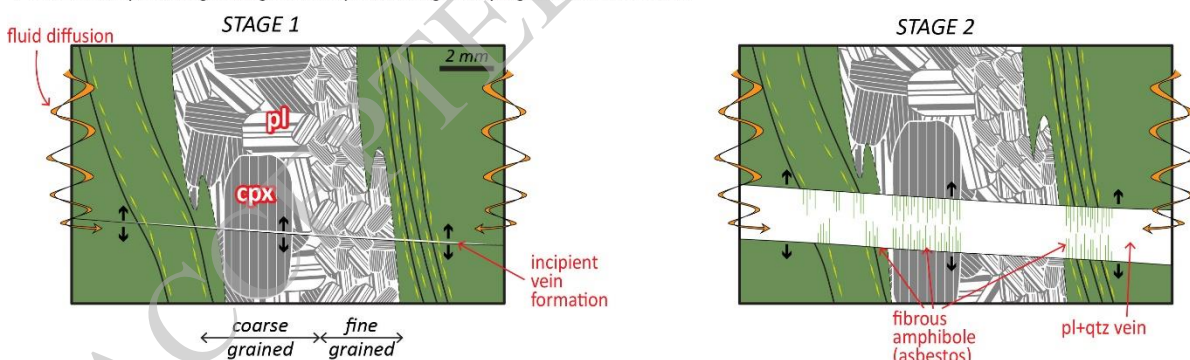


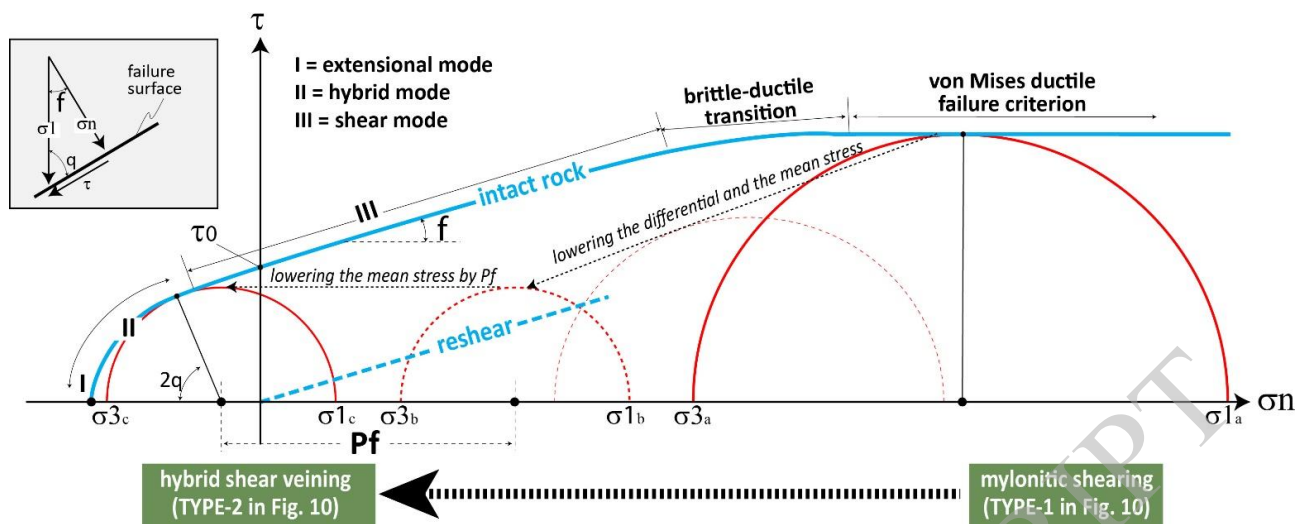


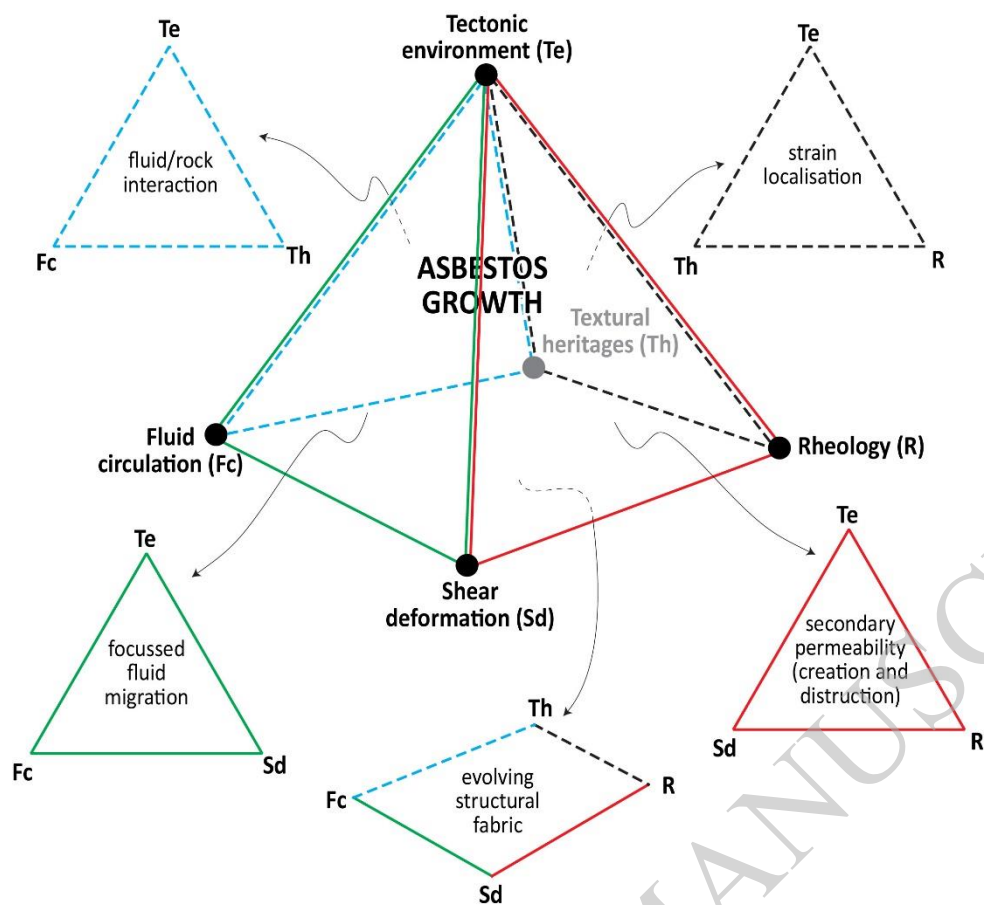
TYPE-1: Amphibole growing during the syn-greenschist fabric



TYPE-2: Amphibole growing in veins post-dating the syn-greenschist foliation







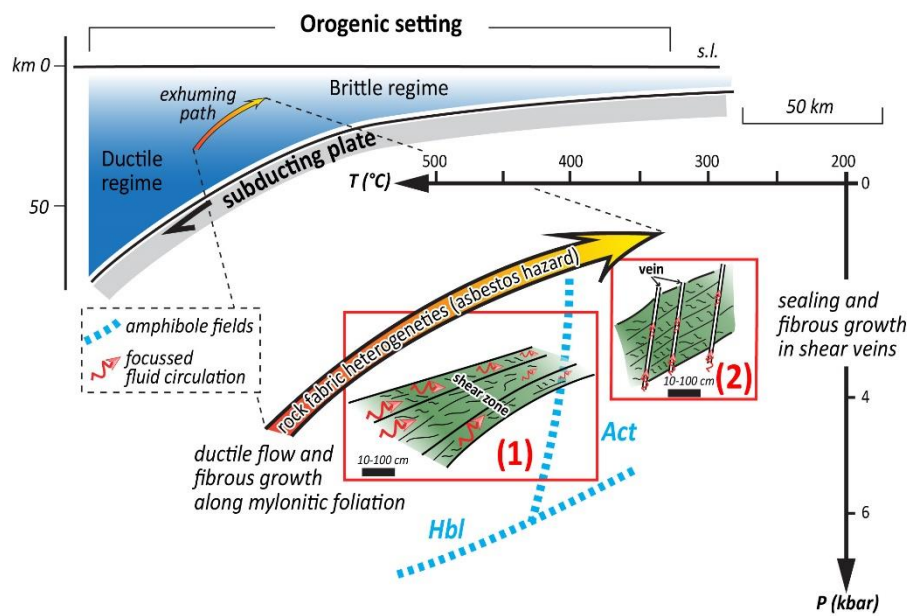


Table 1. Main characteristics of the selected samples.

Sample	Primary fabric (main mineralogical assemblage)	Secondary (tectonic) fabric		
		Rheological regime	Structures	Main mineral assemblage
TB59	Igneous, fine-grained texture (cpx+pl)	Ductile	Syn-greenschist mylonitic foliation; corona structures around cpx grains	pl+am+chl+ep+ilm+ttn+ox
TB61	Relicts of igneous texture, fine-to-coarse-grained texture (cpx+pl)	Ductile-to-semi-brittle	Shear vein	pl+am(+qtz)
TB62	Igneous, coarse-grained texture (cpx+pl)	Semi-brittle	Corona structures around and microcracks in cpx grains	pl+am+chl

am: amphibole; chl: chlorite; cpx: clinopyroxene; ep: epidote; ilm: ilmenite; ox: oxides; pl: plagioclase; qtz: quartz; ttn: titanite

Table 2. Chemical composition of the selected analysed amphiboles.

Micro-texture	in corona structures				along syn-greenschist foliation		in veins post-dating the greenschist foliation
Sample	TB59		TB62		TB59		TB61
	actinolite	magnesio hornblende	actinolite	magnesio hornblende	actinolite	magnesio hornblende	actinolite
SiO ₂	55.03	47.10	54.09	48.44	54.29	48.44	54.98
TiO ₂	0.01	0.46	0.02	0.95	0.00	0.01	0.02
Al ₂ O ₃	1.61	4.14	2.16	4.14	1.04	3.87	1.15
Cr ₂ O ₃	0.04	0.00	0.00	0.03	0.00	0.03	0.00
FeO	7.53	11.26	11.92	7.85	5.78	7.26	8.95
MnO	0.15	0.12	0.09	0.16	0.07	0.07	0.11
MgO	18.79	14.17	16.74	16.01	17.97	17.33	16.15
CaO	12.37	10.53	11.95	11.06	11.69	10.53	11.76
Na ₂ O	0.58	1.28	0.52	1.24	0.23	0.25	0.23
K ₂ O	0.08	0.08	0.07	0.13	0.00	0.02	0.05
H ₂ O*	2.10	2.02	2.10	2.05	2.10	2.09	2.08
Total	98.29	97.32	99.66	97.66	98.21	97.83	99.14
Si	7.85	6.98	7.73	6.95	7.71	6.95	7.82
Ti	0.00	0.05	0.00	0.10	0.00	0.00	0.00
Al	0.27	0.71	0.36	0.71	0.17	0.64	0.20
Cr	0.01	0.00	0.00	0.00	0.00	0.00	0.00
Fe ³⁺	0.02	0.23	0.16	0.44	0.00	0.06	0.00
Fe ²⁺	0.88	0.89	1.27	0.31	0.62	0.31	1.06
Mn ²⁺	0.02	0.02	0.01	0.02	0.01	0.01	0.01
Mg	3.99	3.13	3.57	3.49	3.78	3.69	3.47
Ca	1.89	1.63	1.83	1.73	1.77	1.60	1.78
Na	0.16	0.36	0.14	0.34	0.06	0.07	0.06
K	0.01	0.01	0.01	0.02	0.00	0.00	0.01
Tot. Cat.	15.09	15.20	15.09	15.20	15.03	15.04	15.04
Ca/(Na+B)	1.97	1.85	1.90	1.91	1.92	1.64	1.91
Mg/(Mg+Fe ₂)	0.82	0.73	0.74	0.78	0.79	0.82	0.71

* Calculated assuming OH = 2 atoms per unit formula